General Disclaimer

One or more of the Following Statements may affect this Document

- This document has been reproduced from the best copy furnished by the organizational source. It is being released in the interest of making available as much information as possible.

- This document may contain data, which exceeds the sheet parameters. It was furnished in this condition by the organizational source and is the best copy available.

- This document may contain tone-on-tone or color graphs, charts and/or pictures, which have been reproduced in black and white.

- This document is paginated as submitted by the original source.

- Portions of this document are not fully legible due to the historical nature of some of the material. However, it is the best reproduction available from the original submission.

AMPEX

DYNAMIC ANALYSIS OF A THREE-FOIL ROTOR SUPPORT SYSTEM IN ZERO GRAVITY ENVIRONMENT

RR 69-12

September 1, 1969

15

Ampex Corporation
Research and Advanced Technology Division

UNCLASSIFIED

Prepared under

Contract No. Nonr-3815(00) (X)

Supported jointly by

Department of Defense
Atomic Energy Commission
National Aeronautics and
Space Administration

Administered by

S. Doroff
Fluid Dynamics Branch
Office of Naval Research
Department of the Navy

DYNAMIC ANALYSIS OF A THREE-FOIL ROTOR SUPPORT SYSTEM IN ZERO GRAVITY ENVIRONMENT

Prepared by: A. Eshel
A. Eshel
Member of the Research Staff

Approved by: P. Szego
P. Szego
Manager, Mechanics Section

Approved by:
W. A. Gross
Vice President, Research &
Advanced Technology
Director of Research

ABSTRACT

The dynamic and static behavior of a gas lubricated bearing, consisting of stretched foil sectors, is analyzed. General equations describing the fluid film and valid for shaft excursions of the order of the clearance, are derived on the basis of planar motion and negligible fluid inertia. The analysis is then specialized to the case of a bearing consisting of three equally spaced foil sectors. For the static equilibrium condition, tensions and gaps are calculated and graphs are presented. For the dynamic case, the basic equations are linearized, and equations for the in-and out-of-phase steady-state response to sinusoidal excitation are derived. This serves as an illustration of foil-bearing dynamic behavior as well as for stability investigation. For the case of zero radial load, the effects of speed, rotor radius, foil thickness, wrap angle and initial tension on the coefficients of damping and stiffness are graphically presented.

Within the range of parameters investigated, the following distinct characteristics of the foil bearing have been found:

a. The bearing is stable.
b. The stiffness coefficient is not sensitive to half frequency excitation nor to excitation at any other frequency.
c. The damping coefficient assumes nearly zero values whenever the ratio of frequency of excitation to frequency of rotation is an integral multiple of π/Θ, where Θ is the wrap angle.
d. In contrast with other fluid-film bearings, the increase in mass has no unstabilizing effect.

ACKNOWLEDGEMENTS

The motivation and some of the ideas embodied in this report stem from work done under Contract No. NASW-1456 for the National Aeronautics and Space Administration which has been reported in reference [10].

Thanks are due to Mrs. B. Kember for programming assistance and to Dr. L. Licht, Mr. M. Wildmann and Mr. P. Szego for many illuminating discussions.

CONTENTS

NOMENCLATURE

a	Distance between rotor center "O" and line connecting points of tangency with the guides (Fig. 2)
A_{ik}, A_{ek}	Zeroth approximation of the perturbations of α_{ik}, α_{ek} (Eq.11) from their no load, zero-velocity values.
A_j	Arbitrary integration constants
b	Distance between points of tangency of foil guides (Fig. 2)
B	Normalized form of β; $B = \beta/\epsilon^{1/3}$
c	Damping coefficient
C_k	Compressibility parameter of k^{th} foil sector, $C_k = p_a/(T_k/r_o)$
d	Foil thickness
D	Out-of-phase component of tension transfer function (Eq. 31)
E	Young's modulus
e	Subscript referring to the exit region; also eccentricity
f	Frequency of excitation
f_k	Clearance perturbation of k^{th} foil sector (Eq. 23a)
$\hat{f}_k$	Laplace transform of f_k
f_{ik}, f_{ek}	Perturbation of asymptote displacement of k^{th} foil in the inlet and exit regions
F_x, F_y	Components of resultant force of foil support system on the rotor

NOMENCLATURE (Cont)

h	Foil-bearing clearance
$h_k(\theta, t)$	Clearance distribution of the k^{th} foil segment
h_{ik}, h_{ek}	Distance of k^{th} foil asymptote to rotor in inlet and exit regions
h^*_k	Clearance in uniformity region of k^{th} foil sector
$H_s(\xi)$	Steady state dimensionless clearance
$H_k(\xi, \tau)$	Dimensionless clearance of k^{th} foil sector $H_k = h_k/r_o (6\mu U/T_s)^{2/3}$
H_{ik}, H_{ek}	Dimensionless distance of the k^{th} foil asymptote to rotor
H^*_k	Dimensionless clearance in uniformity region of k^{th} foil sector
i	Subscript referring to the inlet region
j	Integral number of perturbation wavelengths in central region
k	Bearing stiffness per unit width. Also subscript referring to k^{th} foil sector.
K	In-phase component of tension transfer function (Eq. 31)
L_{ik}, L_{ek}, L_k	Zeroth order approximation of perturbations in ℓ_{ik}, ℓ_{ek}, ℓ_k respectively
ℓ_k	Total foil length between points of tangency with foil guides
ℓ_o	Magnitude of foil length ℓ_k when tension is T_o.
ℓ_{ik}, ℓ_{ek}	Partial foil length, defined in Fig. 2

NOMENCLATURE (Cont)

m	Rotor mass, per unit width of foil; also root of characteristic equation
m_c	Critical rotor mass (Eq. 45)
M_k	Moment of k^{th} foil on shaft
n	Number of foil sectors of multisector foil bearing
O	Position of rotor center at zero speed and no radial load (Fig.2)
p	Local film pressure, absolute
p_a	Ambient pressure, absolute
P_u	Speed parameter (Eq. 38a)
P_r	Radius parameter (Eq. 38b)
P_ℓ	Length parameter (Eq. 38c)
P_T	Tension parameter (Eq. 38d)
P_c	Dimensionless damping per unit width (Eq. 38g)
P_h	Dimensionless gap (Eq. 38e)
P_f	Dimensionless frequency (Eq. 38h)
P_k	Dimensionless stiffness per unit width (Eq. 38f)
P_ω	Frequency ratio (Eq. 38i)
Q_k	Tangential force of k^{th} foil sector on rotor
R_k	Radial force of k^{th} foil sector on rotor
r_o	Radius of rotor

NOMENCLATURE (Cont)

$r_k(\theta,t)$	Polar radial coordinate from shaft center referred to k^{th} foil sector
s	Subscript referring to steady state; also, complex circular frequency (Laplace transform) of k^{th} foil sector (subscript k omitted for simplicity).
t	Time
T_o	Initial tension per unit width of foil
T_s	Steady state tension per unit width of foil
T_k	Tension per unit width of k^{th} foil segment
$\overline{T}$	Dimensionless tension (Eq. 10c)
U	Surface velocity of rotor
x, y	Components of displacement of rotor center (Fig. 1)
x_k, y_k	Component of displacement of rotor center in the k^{th} auxiliary coordinate system (Fig. 2)
X_k, Y_k	Dimensionless coordinates (Eqs. 10f, 10g)
α_{ik}	Inlet angle, defined in Fig. 2, referred to the k^{th} foil sector
α_{ek}	Exit angle, defined in Fig. 2, referred to the k^{th} foil sector
β	Arbitrary angle at which solution of foil bearing equation is matched with a straight line (Fig. 2)
ϵ_k	Foil bearing number $\epsilon_k = 6\mu U/T_{sk}$ for k^{th} foil sector

NOMENCLATURE (Cont)

θ	Angular polar coordinate of k^{th} foil sector. The subscript k is omitted for simplicity
θ_{ik}	Polar coordinate of inlet foil support referred to the k^{th} foil sector
θ_{ek}	Polar coordinate of exit foil support referred to the k^{th} foil sector
Θ	Angle of wrap
μ	Viscosity
ν_k	Dimensionless circular frequency of the k^{th} foil $\frac{2r_o\omega}{U}\epsilon_k^{1/3}$
π	Dimensionless pressure (Eq. 10b)
ω_k	Tension perturbation of k^{th} foil sector (Eq. 23b)
ψ_x, ψ_y	Perturbations of resultant force components on shaft
ρ_a	Density of lubricating fluid at ambient pressure
τ	Dimensionless time of k^{th} foil sector. The subscript k is omitted for simplicity (Eq. 10e)
ξ	"Stretched" coordinate $\xi = \frac{\theta}{(6\mu U/T_s)^{1/3}}$ of k^{th} foil sector. Subscript k is omitted for simplicity.
ζ	Shaft position perturbation in x direction
ζ_k	Shaft position perturbation in x_k direction
η	Shaft position perturbation in y direction
η_k	Shaft position perturbation in y_k direction
ω	Circular frequency of excitation

1.0 INTRODUCTION

In many applications, in which thin webs are transported over guides, it has been found advantageous to support the web over a thin fluid film. Several analytical and experimental investigations have been devoted to gaining an understanding of associated phenomena. References [1 - 8]* describe representative works in this area. These works have largely been motivated by problems arising in the computer and tape recording industries.

The converse problem of supporting a high speed rotor on flexible foils has not received, however, much attention. At a first thought, such a bearing may perhaps seem impractical for not providing sufficient shaft restraint. Further considerations, however, reveal that in certain applications the foil bearing offers potential advantages over the usual solid-surface gas-bearings, while shaft confinement can be brought within acceptable limits. Two anticipated advantages motivated the undertaking of research in this area. First, it was intuitively expected that "half frequency" whirl, which generally plagues gas bearings, would be absent in foil bearings [9]. Second, self aligning characteristics, resulting from the flexibility of the surface, were envisaged. The absence of half frequency whirl in a weightless environment would offer the all-important advantage of stability while the self-aligning and distortion - accommodating properties of the foil bearing would make it particularly useful as a support for high-temperature, high-speed turbomachinery.

---

*Numbers in parentheses refer to list of references.

With the impetus given by these expectations, an experimental and analytical effort to study the characteristics of a foil rotor support was carried out and reported in [10]. The analysis in [10], however, was limited by certain approximations, the most important of which was the assumption of quasi-static film behavior. It is the purpose of the present paper to present a more fundamental analysis, which includes the dynamic behavior of the fluid film.

The analysis will be restricted to the planar case, and it will be assumed that the conditions for the validity of Reynolds' equation exist. This implies, as is well known, the neglect of fluid inertia effects. The foil will be considered perfectly flexible and massless, and the foil tension will be taken as time-dependent, but spatially uniform. The problem will first be formulated in general terms and then simplified by retaining only terms of the order of magnitude customarily kept in lubrication studies. The derivation will be carried to its completion only for the case of a rotor supported on three, equally spaced foil sectors, with wrap angles the order of unity. This seems to be case of greatest practical interest. The static characteristics of the system will be investigated on this basis, and the relation between steady-state gap, tension, and shaft position will be found. Then, the dynamics of the system will be studied by means of a linearized small perturbation theory, from which stiffness, damping, and stability characteristics will be deduced. Numerical results will be presented for the zero-gravity case only.

2.0 FORMULATION

Consider n "infinitely wide" foil sectors, spaced at equal angular intervals and supporting a shaft (Fig. 1). In the absence of foil tension, radial load, and fluid film, the shaft center will be located at O. If a tension T_o per unit width of foil is introduced in all foils, the position of the shaft will remain unchanged because of symmetry. The foil length between the supports, at this tension is denoted by ℓ_o. Next, suppose that the shaft is brought up to speed and that air films form between the supporting foils and the shaft. When steady state is reached under rotational conditions, the shaft center-position does not change, but a new foil tension T_s is established. Under load, or unsteady conditions, however, the journal position may shift. Assume that at some instant t the shaft is located at a point x, y (Figs. 1, 2) in terms of a fixed Cartesian system centered at O. Consider, further, a set of n auxiliary coordinate systems x_k, y_k, with an origin at O, such that y_k is directed along the bisector of the k^{th} foil arc away from the foil, and x_k is normal to it. The radial clearance distribution between the k^{th} foil and the shaft will be denoted by

$$h_k(\theta,t) = r_k(\theta,t) - r_o \qquad (1)$$

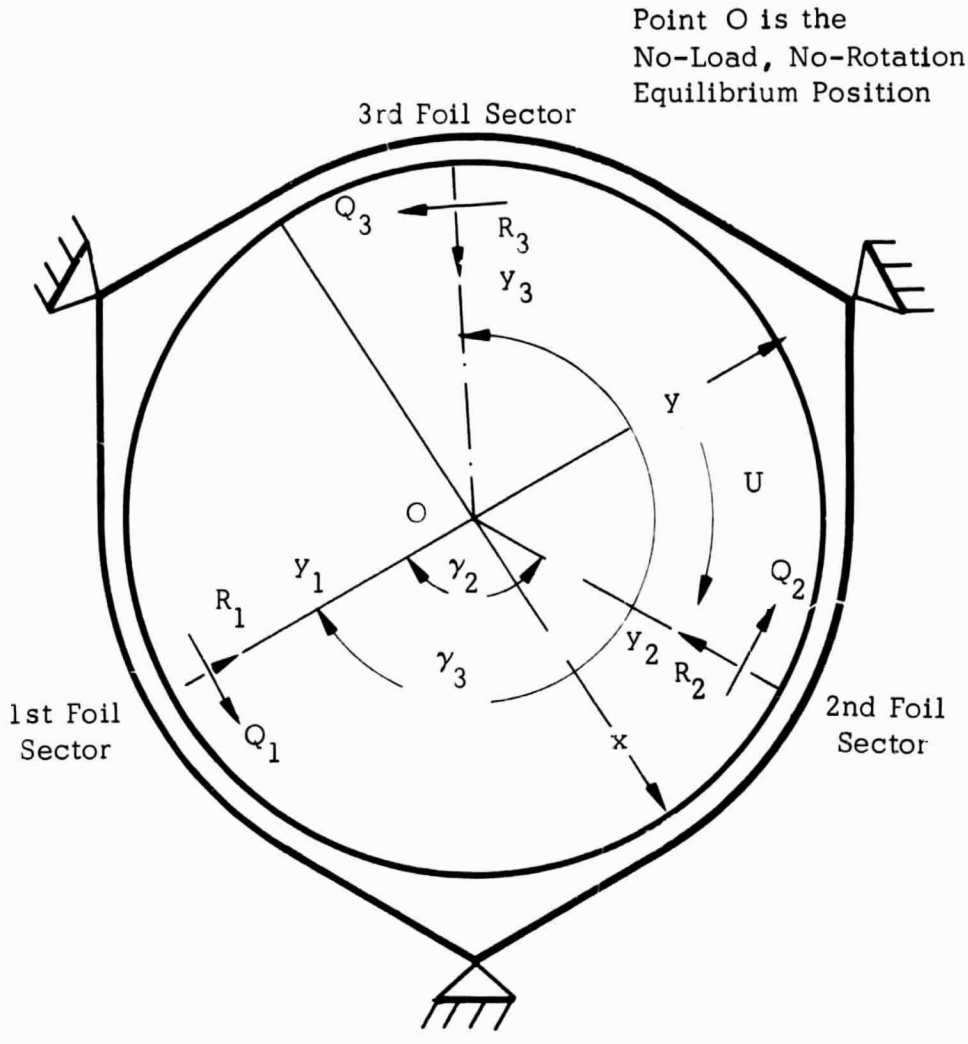

Fig. 1 Schematic Diagram of Foil Bearing Configuration

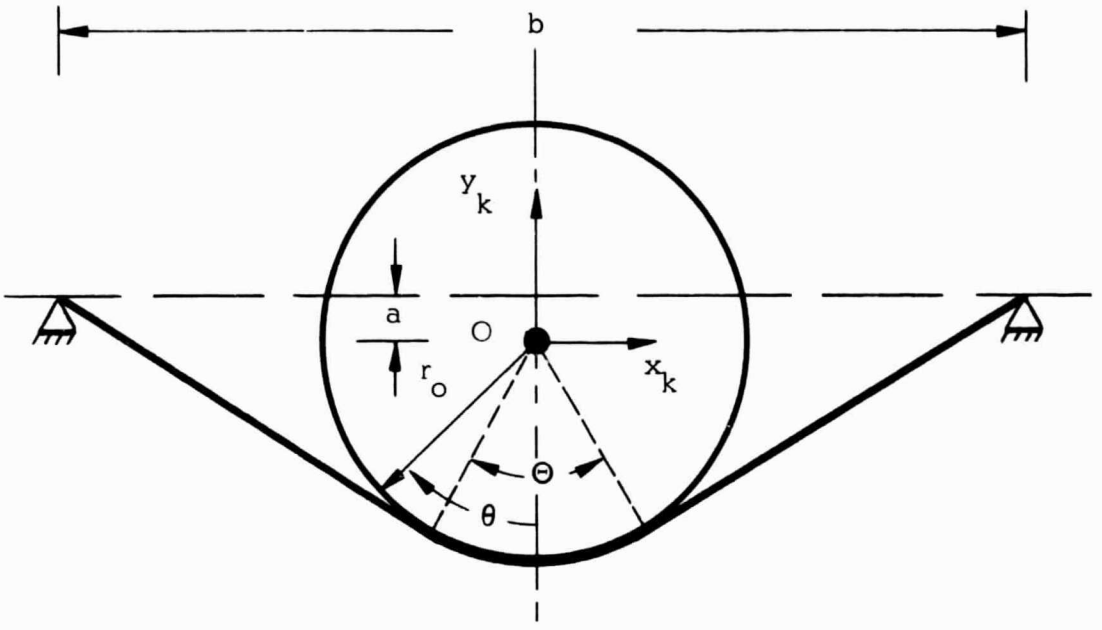

Shaft at Origin O. No-Rotation Condition

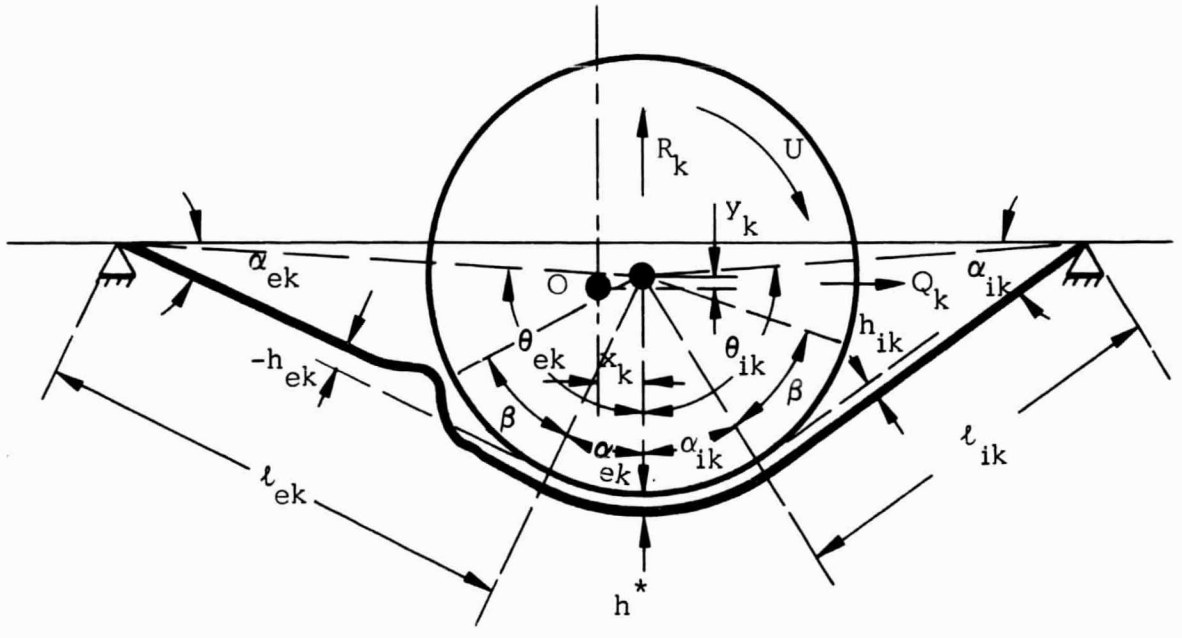

Shaft Displaced From O to (x_k, y_k)

Fig. 2 Schematic Diagram of a Single Foil Sector

where (r, θ) are nonrotating polar coordinates with an origin attached to and translating with the shaft center. The reference for measuring θ is the bisector of the wrap angle of the foil sector under consideration.*

In the following, the problem of finding the bearing forces on the shaft for a given position x, y and for a given clearance distribution $h_k(\theta, t)$, will be formulated. This system of equations will then be supplemented by the relations necessary to find x, y, and h, i.e., the equations of motion and Reynolds equation.

The angle between the k^{th} and first support sectors is

$$\gamma_k = \frac{2\pi}{n}(k-1) \tag{2}$$

The coordinates x_k, y_k can be expressed in terms of x, y by the relations

$$x_k = x \cos\gamma_k + y \sin\gamma_k \tag{3a}$$

$$y_k = -x \sin\gamma_k + y \cos\gamma_k \tag{3b}$$

---

* To simplify the notation only dependent variables will be subscripted with k. It should be understood that the independent variable e.g. θ, corresponds to the same foil sector.

At time t, the resultant force of the k^{th} foil sector on the shaft may be resolved into two components R_k in the radial direction (y_k), and Q_k in the tangential direction (x_k). In addition there will be a frictional torque M_k. These components are expressed in terms of the tension $T_k(t)$ by

$$R_k(t) = T_k(t)\left(\sin \alpha_{ik} + \sin \alpha_{ek}\right) \tag{4a}$$

$$Q_k(t) = T_k(t)\left(\cos \alpha_{ik} - \cos \alpha_{ek}\right) \tag{4b}$$

$$M_k(t) = T_k(t)\left(h_{ik} - h_{ek}\right) \tag{4c}$$

Here the subscripts i and e denote the inlet and exit regions. The resultant force and torque of the whole system on the shaft can be expressed in terms of the individual foil forces and torques, as follows:

$$F_x(t) = -\sum_{k=1}^{n} R_k(t) \sin \gamma_k + \sum Q_k(t) \cos \gamma_k \tag{5a}$$

$$F_y(t) = \sum_{k=1}^{n} R_k(t) \cos \gamma_k + \sum Q_k(t) \sin \gamma_k \tag{5b}$$

$$M(t) = \sum_{k=1}^{n} M_k(t) \tag{5c}$$

The length of the k^{th} foil can be given in terms of the corresponding clearance distribution by

$$\ell_k = \int_{-\theta_{ik}(t)}^{\theta_{ek}(t)} \left\{ \left[r_o + h_k(\theta, t) \right]^2 + \left(\frac{\partial h_k}{\partial \theta} \right)^2 \right\}^{1/2} d\theta \tag{6}$$

where $\theta_{ik}(t)$, $\theta_{ek}(t)$ are the instantaneous polar coordinates of the inlet and exit points of support of the k^{th} foil (Fig. 2).

The instantaneous tension in the k_{th} foil is given by the stress-strain relation

$$\frac{T_k(t) - T_o}{Ed} = \frac{\ell_k - \ell_o}{\ell_o} \tag{7}$$

where E is the modulus of elasticity and d denotes the foil thickness.

Finally, the following geometrical relations will complete the formulation

$$\frac{b}{2} - x_k = \ell_{ik} \cos \alpha_{ik} + (r_o + h_{ik}) \sin \alpha_{ik} \tag{8a}$$

$$\frac{b}{2} + x_k = \ell_{ek} \cos \alpha_{ek} + (r_o + h_{ek}) \sin \alpha_{ek} \tag{8b}$$

$$a - y_k = \ell_{ik} \sin \alpha_{ik} - (r_o + h_{ik}) \cos \alpha_{ik} \tag{8c}$$

$$a - y_k = \ell_{ek} \sin \alpha_{ek} - (r_o + h_{ek}) \cos \alpha_{ek} \qquad (8d)$$

To summarize, for a given shaft position x, y, (either prescribed or found from the equations of motion) and for a given clearance (found from the elasto-hydrodynamic equations) the set of 11n + 3 equations (3 - 8) can be solved for the unknowns F_x, F_y, M; x_k, y_k, R_k, Q_k, M_k, T_k, α_{ik}, α_{ek}, ℓ_{ik}, ℓ_{ek}, ℓ_k, where k = 1...n.

3.0 SIMPLIFICATIONS

It is well to recall at this point certain aspects of previous foil-bearing studies. The most important foil-bearing characteristic is the small parameter $\epsilon_k = 6\mu U/T_{sk}$, in which the subscript s refers to the steady state conditions. In reference [11], equations were derived, of which the following constitute the zeroth order terms of expansions in power of $\epsilon_k^{2/3}$

$$\pi_k = \bar{T}_k \left(1 - \frac{\partial^2 H_k}{\partial \xi^2}\right) \tag{9a}$$

$$-\bar{T}_k \frac{\partial}{\partial \xi}\left\{H_k^3 \frac{\partial^3 H_k}{\partial \xi^3}\left[\bar{T}_k\left(1 - \frac{\partial^2 H_k}{\partial \xi^2}\right) + C_k\right]\right\} = \tag{9b}$$

$$= \frac{\partial}{\partial \xi}\left\{H_k\left[\bar{T}_k\left(1 - \frac{\partial^2 H_k}{\partial \xi^2}\right) + C_k\right]\right\} + \frac{\partial}{\partial \tau}\left\{H_k\left[\bar{T}_k\left(1 - \frac{\partial^2 H_k}{\partial \xi^2}\right) + C_k\right]\right\}$$

where H_k, π_k, $\bar{T}_k$ denote the zeroth order approximation of the dimensionless clearance, pressure and tension.

$$\frac{h_k(\theta,t)}{r_o\,\epsilon_k^{2/3}} = H_k(\xi,\tau) + O(\epsilon_k^{2/3}) \tag{10a}$$

$$\frac{p_k(\theta,t) - p_a}{T_{sk}/r_o} = \pi_k(\xi,\tau) + O(\epsilon_k^{2/3}) \tag{10b}$$

$$\frac{T(t)}{T_{sk}} = \bar{T}_k(\tau) + O(\epsilon_k^{2/3}) \tag{10c}$$

$$\theta \cdot \epsilon_k^{-1/3} = \xi \tag{10d}$$

$$t \frac{U}{2r_o} \epsilon_k^{-1/3} = \tau \tag{10e}$$

The above equations describe the clearance and pressure distributions in the planar, perfectly flexible foil-bearing and will be applied to the foil sectors k = 1...n. In the following derivation, shaft motions the order of the clearance will be allowed. Here, it will be consistent to define dimensionless shaft perturbations of order unity and to expand them in powers of $\epsilon^{2/3}$. When X_k, Y_k denote zeroth order approximations:

$$\frac{x_k}{r_o} \epsilon_k^{-2/3} = X_k + O(\epsilon_k^{2/3}) \tag{10f}$$

$$\frac{Y_k}{r_o} \epsilon_k^{-2/3} = Y_k + O(\epsilon_k^{2/3}) \tag{10g}$$

The next step is to make similar expansions in powers of $\epsilon_k^{2/3}$ for the deviations of the foil angles and foil length from their values under no-load, zero velocity conditions. Again, capital letters refer to the zeroth order approximation.

$$\frac{\alpha_{ik}(t) - \Theta/2}{\epsilon_k^{2/3}} = A_{ik}(\tau) + O(\epsilon_k^{2/3}) \tag{11a}$$

$$\frac{\ell_{ik}(t) - (\ell_o - \Theta r_o)/2}{r_o \epsilon_k^{2/3}} = L_{ik}(\tau) + O(\epsilon_k^{2/3}) \tag{11b}$$

Analogous relations can be used for the exit region, denoted with the subscript e. In addition

$$\frac{\ell_k(t) - \ell_o}{r_o \epsilon^{2/3}} = L_k(\tau) + O(\epsilon_k^{2/3}) \tag{11c}$$

In the above relations, A_{ik}, A_{ek}, L_{ik}, L_{ek}, L_k denote zeroth order approximating terms. Substituting Eqs. (11) into Eqs. (8) and collecting terms of equal powers of $\epsilon_k^{2/3}$ one finds (coefficient of $\epsilon_k^{\,o}$):

$$\frac{b}{2r_o} = \frac{\ell_o/r_o - \Theta}{2} \cos\frac{\Theta}{2} + \sin\frac{\Theta}{2} \tag{12a}$$

$$\frac{a}{r_o} = \frac{\ell_o/r_o - \Theta}{2} \sin\frac{\Theta}{2} - \cos\frac{\Theta}{2} \tag{12b}$$

and (coefficient of $\epsilon_k^{2/3}$)

$$-X_k = L_{ik} \cos\frac{\Theta}{2} + A_{ik}\left(\cos\frac{\Theta}{2} - \frac{\ell_o/r_o - \Theta}{2}\sin\frac{\Theta}{2}\right) + H_{ik}\sin\frac{\Theta}{2} \tag{13a}$$

$$X_k = L_{ek}\cos\frac{\Theta}{2} + A_{ek}\left(\cos\frac{\Theta}{2} - \frac{\ell_o/r_o - \Theta}{2}\sin\frac{\Theta}{2}\right) + H_{ek}\sin\frac{\Theta}{2} \qquad (13b)$$

$$-Y_k = L_{ik}\sin\frac{\Theta}{2} + A_{ik}\left(\sin\frac{\Theta}{2} + \frac{\ell_o/r_o - \Theta}{2}\cos\frac{\Theta}{2}\right) - H_{ik}\cos\frac{\Theta}{2} \qquad (13c)$$

$$-Y_k = L_{ek}\sin\frac{\Theta}{2} + A_{ek}\left(\sin\frac{\Theta}{2} + \frac{\ell_o/r_o - \Theta}{2}\cos\frac{\Theta}{2}\right) - H_{ek}\cos\frac{\Theta}{2} \qquad (13d)$$

Using Eq. (13) one can deduce the relations:

$$A_{ik} + A_{ek} = \frac{-2Y_k\cos\frac{\Theta}{2} + H_{ik} + H_{ek}}{\frac{\ell_o/r_o - \Theta}{2}} \qquad (14a)$$

$$L_{ik} + L_{ek} = -2Y_k\sin\frac{\Theta}{2} - (A_{ik} + A_{ek}) \qquad (14b)$$

Given the exact expression of $h_k(\theta, t)$, Eq. (6) represents accurately the foil length. In attempting to expand Eq. (6), however, one must face the fact that what is known as the clearance distribution is merely the principal term of the expansion of $h_k(\theta, t)$. Furthermore, even this representation is valid only in part of the range of the integral in Eq. (6), namely the lubrication zone (see Fig. 2)

$$-(\beta + \alpha_{ik}) < \theta < \beta + \alpha_{ek} \qquad (15)$$

where the magnitude of β is elaborated upon later. Actually, in the exit region of the k^{th} foil, for example, the clearance is described asymptotically by the equation of a straight line:

$$h_k(\theta,t) = \frac{r_o + h_{ek}}{\cos(\theta - \alpha_{ek})} - r_o \tag{16}$$

On the other hand, the clearance in the lubrication zone is described by the solution of Eq. (9). This solution, however, being the principal term of an expansion in powers of $\epsilon_k^{2/3}$, does not approach asymptotically Eq. (16), but rather, the first term of the expansion of Eq. (16) in powers of $\epsilon_k^{2/3}$. The boundaries of the region defined in Eq. (15) consist of the somewhat arbitrary matching points chosen in the common region of validity of Eq. (16) and Eq. (9).

In the evaluation of the foil length from Eq. (6), one must, therefore, take account of different representations of the function $h_k(\theta,t)$ in the asymptotic parts of the inlet and exit regions and in the lubrication zone. Expanding the radical in Eq. (6), one obtains:

$$\begin{aligned}\frac{l_k(t)}{r_o} = {} & \frac{l_{ik}(t)}{r_o} - \left(1 + \frac{h_{ik}}{r_o}\right)\tan\beta \\ & + \int_{-[\alpha_{ik}(t)+\beta]}^{\alpha_{ek}(t)+\beta} \left\{1 + \frac{h_k}{r_o} + \frac{1}{2}\left[\frac{\partial(h_k/r_o)}{\partial\theta}\right]^2 + \dots\right\} d\theta \\ & + \frac{l_{ek}(t)}{r_o} - \left(1 + \frac{h_{ek}}{r_o}\right)\tan\beta\end{aligned} \tag{17}$$

Using the ϵ - expansion in Eq. (17) and making use of Eqs. (11) and (14), Eq. (17) becomes:

$$L_k(\tau) = -2Y_k(\tau)\sin\frac{\omega}{2} + \epsilon_k^{1/3}\int_{-\left(\frac{\omega}{2\epsilon_k^{1/3}}+B\right)}^{\frac{\omega}{2\epsilon_k^{1/3}}+B}\left\{H(\xi,\tau)+\frac{1}{2}\left[\frac{\partial H(\xi,\tau)}{\partial\xi}\right]^2\right\}d\xi \qquad (18)$$
$$-\left[H_{ik}(\tau)+H_{ek}(\tau)\right]B\epsilon_k^{1/3} - \frac{2}{3}B^3\epsilon_k^{1/3}$$

wherein $\tan\beta$ was expanded in a power series and $B = \beta/\epsilon^{1/3}$. It is interesting to note that to the order of approximation considered here, $L_k(\tau)$ is independent of the distance of the guide posts from the shaft. Furthermore, the magnitude of $L_k(\tau)$ is quite insensitive to B, provided B is chosen judiciously. This may be seen from Eq. (18) by considering the effect of increasing B. Bearing in mind that for large ξ, the first terms of the asymptotic representations of $H_k(\xi, \tau)$ [5] are of the form

$$H_k(\xi,\tau) \sim H_{ik}(\tau) + \frac{1}{2}\xi^2 \qquad (19)$$

it follows that added contributions of the integral for large B are cancelled by the last two terms of the equation.

Using Eq. (7), the instantaneous tension can now be found:

$$\frac{T_k(\tau) - T_o}{Ed} = \frac{r_o}{\ell_o}\epsilon_k^{2/3}\left\{-2Y_k(\tau)\sin\frac{\Theta}{2}\right.$$

$$+\epsilon_k^{1/3}\int_{-\left(\frac{\Theta}{2\epsilon_k^{1/3}}+B\right)}^{\frac{\Theta}{2\epsilon_k^{1/3}}+B}\left[H_k(\xi,\tau)+\frac{1}{2}\left(\frac{\partial H_k(\xi,\tau)}{\partial\xi}\right)^2\right]d\xi \qquad (20)$$

$$\left.-\left[H_{ik}(\tau)+H_{ek}(\tau)\right]B\epsilon_k^{1/3}-\frac{2}{3}B^3\epsilon_k^{1/3}\right\}$$

In addition, the steady state tension T_{sk} can also be found from Eq. (20) by substituting the steady state values of the clearance distribution $H_{sk}(\xi)$ and the equilibrium shaft position Y_{sk}.

Equations (4) therefore become

$$R_k(\tau) = T_k(\tau)\left\{2\sin\frac{\Theta}{2}+\cos\frac{\Theta}{2}\,\epsilon_k^{2/3}\left[A_{ik}(\tau)+A_{ek}(\tau)\right]+O\left(\epsilon_k^{4/3}\right)\right. \qquad (21a)$$

$$Q_k(\tau) = T_k(\tau)\,\sin\frac{\Theta}{2}\left[A_{ek}(\tau)-A_{ik}(\tau)\right]\epsilon_k^{2/3}+O\left(\epsilon_k^{4/3}\right) \qquad (21b)$$

When the shaft is displaced toward a foil sector, the radial force R_k is increased by three contributions, namely, increased tension, changes in the angles α_{ik}, α_{ek} and tension differentials due to fluid shear. The first two contributions are included in Eq. (21a). The third contribution has been neglected by virtue of the assumption of spatially uniform tension.* Henceforth, the discussion will be limited to the most important case, i.e., that of $\Theta \sim O(1)$ and n = 3. In this case, the first term of $R_k(\tau)$ is dominant, and the tangential force $(Q_k(\tau)$ is negligible in comparison. Upon substitution of Eq. (21) into Eq. (15) and retaining first order terms only, one finds:

$$F_x(\tau) = \sqrt{3} \sin\frac{\Theta}{2}\left[T_3(\tau) - T_2(\tau)\right] \tag{22a}$$

$$F_y(\tau) = 2 \sin\frac{\Theta}{2}\left[T_1(\tau) - \frac{T_2(\tau)}{2} - \frac{T_3(\tau)}{2}\right] \tag{22b}$$

To summarize, given the shaft position $X(\tau)$, $Y(\tau)$ (either prescribed or obtained by solving simultaneously the equations of motion) and given $H_k(\xi, \tau)\big|_{\tau=0}$, the set of equations (9) and (20) is used to solve for the clearance distribution $H_k(\xi, \tau)$ and for the tension $T_k(\tau)$ in each foil. The total forces on the shaft can then be found at each instant of time from Eq. (22).

---

*In reference [10] the shear term was found to be of order

$$T_k(\tau) \frac{\Theta}{4} \sin\frac{\Theta}{2} \epsilon_k^{1/3}$$

4.0 LINEARIZED ANALYSIS

The problem described by Eqs. (9a) and (20) can be solved numerically for specific cases. Considerable insight can be gained, however, from a linearized treatment, which is the subject of the present section.

Let it be assumed that a steady state has been established with a given T_{sk}, $H_{sk}(\xi)$, Y_{sk}, Y_{sk} for each foil sector $k = 1, 2, 3$. Now consider small perturbations from this state

$$H_k(\xi,\tau) = H_{sk}(\xi) + f_k(\xi,\tau) \qquad f_k(\xi,\tau) \ll H_{sk}(\xi) \tag{23a}$$

$$T_k(\tau) = T_{sk}\left[1 + \varphi_k(\tau)\right] \qquad \varphi_k \ll 1 \tag{23b}$$

$$X_k(\tau) = X_{sk} + \zeta_k(\tau) \qquad \zeta_k \ll X_{sk} \tag{23c}$$

$$Y_k(\tau) = Y_{sk} + \eta_k(\tau) \qquad \eta_k \ll Y_{sk} \tag{23d}$$

$$F_x(\tau) = F_{xs} + \Psi_x(\tau) \qquad \Psi_x \ll F_{xs} \tag{23e}$$

$$F_y(\tau) = F_{ys} + \Psi_y(\tau) \qquad \Psi_y \ll F_{ys} \tag{23f}$$

Equation (9) was linearized by Barnum and Elrod [12]. The following equation, which is different in form but not in essence, has been used in the present work.

$$\frac{\partial^4 f_k}{\partial \xi^4} F_{40}(\xi) + \frac{\partial^3 f_k}{\partial \xi^3} F_{30}(\xi) + \frac{\partial^2 f_k}{\partial \xi^2} F_{20}(\xi) + \frac{\partial f_k}{\partial \xi} F_{10}(\xi) + f_k F_{00}(\xi) + \frac{\partial^3 f_k}{\partial \xi^2 \partial \tau} F_{21}(\xi) + \frac{\partial f_k}{\partial \tau} F_{01}(\xi) = \frac{d\varphi_k}{d\tau} \Phi_1(\xi) + \varphi_k \Phi_0(\xi) \tag{24}$$

where (with the subscript k omitted)

$$F_{40}(\xi) = -H_s^3 (1 - H_s'' + C)$$

$$F_{30}(\xi) = -3H_s^2 H_s' (1 - H_s'' + C) + 2H_s^3 H_s''' + H_s$$

$$F_{20}(\xi) = 3H_s^2 H_s' H_s''' + H_s^3 H_s^{IV} + H_s'$$

$$F_{10}(\xi) = -(1 + 3H_s^2 H_s'')(1 - H_s'' + C)$$

$$F_{00}(\xi) = -(6H_s H_s' H_s''' + 3H_s^2 H_s^{IV})(1 - H_s'' + C) + 3H_s^2 H_s'''^2 + H_s'''$$

$$F_{21}(\xi) = H_s$$

$$F_{01}(\xi) = -(1 - H_s'' + C)$$

$$\Phi_1(\xi) = (1 - H_s'') H_s$$

$$\Phi_0(\xi) = 6H_s^2 H_s' (1 - H_s'' + \tfrac{C}{2}) H_s'' - 2H_s^3 H_s'''^2 + 2H_s^3 (1 - H_s'' + \tfrac{C}{2}) H_s^{IV} - H_s''' H_s + (1 - H_s'') H_s'$$

With the boundary conditions

$$\frac{\partial f_k}{\partial \xi} \;,\; \frac{\partial^2 f_k}{\partial \xi^2} \longrightarrow 0 \qquad \text{as} \qquad \xi \longrightarrow \pm \infty$$

Eq. (20) becomes

$$\varphi_k \frac{T_{sk}}{Ed} = \frac{r_o}{\ell_o} \epsilon_k^{2/3} \left\{ -2\eta_k \sin\frac{\Theta}{2} + \epsilon_k^{1/3} \int_{-\left(\frac{\Theta}{2\epsilon_k^{1/3}} + B\right)}^{\frac{\Theta}{2\epsilon_k^{1/3}} + B} \left[f_k + \frac{d H_{sk}}{d\xi} \frac{\partial f_k}{\partial \xi} \right] d\xi \right.$$

$$\left. - B\left(f_{ik} + f_{ek}\right) \epsilon_k^{1/3} \right\} \tag{25}$$

Eqs. 22 become

$$\Psi_x = \sqrt{3} \sin\frac{\Theta}{2} \left(\varphi_3 T_{3s} - \varphi_2 T_{2s} \right) \tag{26a}$$

$$\Psi_y = 2 \sin\frac{\Theta}{2} \left(\varphi_1 T_{1s} - \frac{\varphi_2 T_{2s}}{2} - \frac{\varphi_3 T_{3s}}{2} \right) \tag{26b}$$

5.0 SOLUTION

The problem will be attached by the frequency response approach. This technique was previously used for obtaining stability thresholds in solid-bearing problems by Pan [13], Castelli and Elrod [14] and others.

The following notation will be used for the Laplace transform of f

$$\tilde{f}(\xi, s) = \mathcal{L}\left\{ f(\xi, \tau) \right\} = \int_0^\infty e^{-s\tau} f(\xi, \tau)\, d\tau$$

Transforming with zero initial conditions, Eqs. (24) - (26) become

$$\frac{d^4 \tilde{f}_k}{d\xi^4} F_{40}(\xi) + \frac{d^3 \tilde{f}_k}{d\xi^3} F_{30}(\xi) + \frac{d^2 f}{d\xi^2}\left[F_{20}(\xi) + s F_{21}(\xi) \right] +$$

$$\frac{d\tilde{f}_k}{d\xi} F_{10}(\xi) + \tilde{f}_k \left[F_{00}(\xi) + s F_{01}(\xi) \right] = \tilde{\varphi}_k \left[\Phi_0(\xi) + s \Phi_1(\xi) \right] \qquad (27a)$$

With the boundary conditions that for $\xi \rightarrow \pm \infty$

$$\frac{d\tilde{f}_k}{d\xi}, \frac{d^2 \tilde{f}_k}{d\xi^2} \rightarrow 0 \qquad (27b)$$

$$\tilde{\varphi}_k \frac{T_{sk}}{Ed} = \frac{r_o}{\ell_o} \epsilon_k^{2/3} \left\{ -2\tilde{\eta}_k \sin\frac{\Theta}{2} + \right.$$

$$\left. \int_{-\left(\frac{\Theta}{2\epsilon_k^{1/3}} + B\right)}^{\frac{\Theta}{2\epsilon_k^{1/3}} + B} \left[\tilde{f}_k + \frac{dH_{sk}}{d\xi} \frac{d\tilde{f}_k}{d\xi} \right] d\xi - B\left(\tilde{f}_{ik} + \tilde{f}_{ek}\right) \epsilon_k^{1/3} \right. \tag{28}$$

$$\tilde{\Psi}_x = \sqrt{3} \sin\frac{\Theta}{2} \left(\tilde{\varphi}_3 T_{s3} - \tilde{\varphi}_2 T_{s2} \right) \tag{29a}$$

$$\tilde{\Psi}_y = 2\sin\frac{\Theta}{2} \left(\tilde{\varphi}_1 T_{s1} - \frac{\tilde{\varphi}_2 T}{2} - \frac{\tilde{\varphi}_3 T_{s3}}{2} \right) \tag{29b}$$

It may be observed that Eq. (27a), subject to the boundary conditions (27b), can be solved independently of Eqs. (28) and (29) in terms of the clearance transfer function (clearance $\tilde{f}_k$ as output with tension $\tilde{\varphi}_k$ as input)

$$\tilde{h}_k(\xi, s) = \frac{\tilde{f}_k(\xi, s)}{\tilde{\varphi}_k(s)} \tag{30}$$

It is also to be noted that since $\tilde{h}_k$ depends upon the physical parameters $p_a/(T_{sk}/r_o)$ and $\Theta/\epsilon_k^{1/3}$, $\tilde{h}_k$ varies in general from one foil sector to another (hence, the subscript k).

When $\tilde{h}_k(\xi, s)$ is available, the tension transfer function (tension $\tilde{\varphi}_k$ as output with component of journal displacement $\tilde{\eta}_k$ as input) of the k^{th} foil to the shaft excursion can be found from Eq. (28):

$$\frac{\tilde{\varphi}_k(s)}{\tilde{\eta}_k(s)} = \frac{2 \sin \frac{\Theta}{2}}{-\frac{T_{sk}}{Ed}\frac{l_o}{r_o}\epsilon_k^{-2/3} + \epsilon_k^{1/3}\int_{-[\Theta/(2\epsilon_k^{1/3})+B]}^{\Theta/(2\epsilon_k^{1/3})+B}\left[\tilde{h}_k + \frac{dH_{sk}}{d\xi}\frac{d\tilde{h}_k}{d\xi}\right]d\xi + B\epsilon^{1/3}(\tilde{h}_{ik}+\tilde{h}_{ek})} \tag{31}$$

Finally, by substituting Eq. (31) into Eq. (29), the transformed bearing forces $\tilde{\psi}_x$, $\tilde{\psi}_y$ can be found in terms of $\tilde{\eta}(s)$, $\tilde{\zeta}(s)$ and the physical parameters. Bearing in mind the zero initial conditions assumed for the film in conjunction with Eq. (27a), one may use the formulation to solve the initial value problem of a rotor released from a state of equilibrium (i.e. zero initial values of ζ, η, $\dot{\zeta}$, $\dot{\eta}$). Alternatively, one may solve for the asymptotic steady state response of the rotor to periodic excitation. In the latter case it is assumed that the film transients die out and do not contribute to instability, if any [13].

The task pursued here will be to find the stability threshold, in the course of which the damping and stiffness coefficients as functions of frequency will be obtained. The first step of the procedure is to assign a zero value to the real part of the complex frequency and to prescribe the imaginary part $i\omega$. This is tantamount to the imposition of a prescribed sinusoidal motion at a frequency ω on the journal. Then, the in- and out-of phase steady state response of the three-foil system is found as a function of frequency. This response can be substituted into the equations of motion and one of the dynamic parameters, usually the rotor's mass can be

found at the threshold of instability from the characteristic equation. It is to be noted that the actual frequency is to be interpreted as excitation of each bearing sector at a dimensionless frequency of $\nu_\kappa = 2r_o \omega \epsilon_k^{1/3}/U$.

With the solution of Eqs. (27a,b) the right hand side of Eq.(31) is a complex number denoted by $K_k + D_k i$, which can be determined for any frequency and a given set of physical parameters. This number depends neither on the journal excursion from the equilibrium position nor its velocity.

Evaluation of the results will be limited in this report to the case of zero gravity, i.e, of no radial load. In this case the tensions and the parameters K, D are equal for all three foils. Bearing this in mind, and using Eq. (3b), Eq. (31) gives the tension perturbations in each foil sector:

$$\tilde{\varphi}_1 = (K + Di)\tilde{\eta} \tag{32a}$$

$$\tilde{\varphi}_2 = (K+Di)\left(-\frac{\sqrt{3}}{2}\tilde{\zeta} - \frac{\tilde{\eta}}{2}\right) \tag{32b}$$

$$\tilde{\varphi}_3 = (K+Di)\left(\frac{\sqrt{3}}{2}\tilde{\zeta} - \frac{\tilde{\eta}}{2}\right) \tag{32c}$$

Substitution of Eq. (32) into Eq. (29) results in

$$\tilde{\psi}_x = 3 \sin\frac{\Theta}{2}\,(K+Di)\,T_s\,\tilde{\zeta} \tag{33a}$$

$$\tilde{\psi}_y = 3 \sin\frac{\Theta}{2} (K + Di) T_s \tilde{\eta} \tag{33b}$$

By analogy to spring-dashpot system, one finds that in the absence of radial load the bearing is isoelastic and that the stiffness and damping coefficients are then given by:

$$k = -3 \sin\frac{\Theta}{2} K T_s \epsilon^{-2/3} / r_o \tag{34}$$

$$c = -3 \sin\frac{\Theta}{2} D T_s \epsilon^{-2/3} / (\omega r_o) \tag{35}$$

The procedure of solution can be summarized as follows:

(1) For a given geometrical arrangement, initial tension and rotational speed, or the corresponding dimensionless parameters (see Eq. (39) below), find the equilibrium tension.

This requires a complicated iteration in Eq.(20), since the gap is related to the actual tension through the parameters $6\mu U/T_s$ and $p_a r_o/T_s$, while the tension is tied to the length of the foil, which in itself is a function of the gap distribution. Two additional factors cause the solution to be laborious. The inlet and exit equilibrium solutions are solved separately, while the matching of the inlet and exit values of H^* is accomplished by trial and error [5]. Furthermore, the roots of the characteristic equation are also functions of $p_a r_o/T_s$, i.e., of the steady-state tension.

(2) For a given equilibrium state, solve for the complex response of the perturbed film equations (27a) to sinusoidal tension excitation. This part of the problem has been solved by Barnum and Elrod [12]*. It involves the following steps.

(a) Obtain the roots of the characteristic equation of (27a) in the uniformity region, as a function of frequency.

(b) Obtain, for the inlet region, linearily independent homogeneous solutions and a particular integral.

(c) Superpose these solutions to fit the inlet boundary conditions.

(d) Repeat (b) and (c) for the exit region.

(3) Having established a relation between the tension perturbations and the film behavior, use Eq. (31) to find the corresponding shaft perturbations. Here complex foil-length perturbations are required and are obtained from integration of the results arrived at in step (2).

(4) Finally, find the stiffness and the damping coefficients from Eq. (34) and (35).

---

*Further details are discussed in Appendix B

6.0 RESULTS AND CONCLUSIONS

Using Eq. (20), the steady state tension can be expressed in the form

$$T_{sk} = T_{sk}(r_o, l_o, \Theta, U, \mu, T_o, p_a, E, d, \rho_a, y_{sk}) \qquad (37a)$$

Although the density ρ_a does not appear in the formulation, it is included here since the dimensionless groups are designed to include inertia effects in anticipation of future studies. The bearing stiffness coefficient in the zero gravity condition ($x_s = y_s = 0$) can be expressed by means of Eqs. (34, 35) in the form

$$k = k(r_o, l_o, \Theta, U, \mu, T_o, p_a, E, d, \rho_a, \omega) \qquad (37b)$$

The damping coefficient c depends on the same parameters as the stiffness.

In order to simplify the presentation of the results, the parameters were incorporated into dimensionless groups. The number of parameters is, nevertheless, too large for the presentation of a complete parametric map. More limited objectives, therefore, have been set in planning the graphical presentation. The effects of varying speed, radius, initial tension, extension characteristics and wrap angle appear to be the most important variables for geometrically similar bearings. The foregoing consideration is reflected in the choice of the dimensionless variables used in presenting the numerical results.

Following reference [10], the dimensionless groups involved are

$$P_u = \frac{U}{\sqrt{p_a/\rho_a}} \qquad \text{Speed parameter} \qquad (38a)$$

$$P_r = \frac{r_o}{\mu/\sqrt{\rho_a p_a}} \qquad \text{Radius parameter} \qquad (38b)$$

$$P_\ell = \frac{r_o}{\ell_o}\frac{Ed}{\sqrt{\mu^2 p_a/\rho_a}} \qquad \text{Length parameter} \qquad (38c)$$

$$P_T = \frac{T}{\sqrt{\mu^2 p_a/\rho_a}} \qquad \text{Tension parameter} \qquad (38d)$$

$$P_h = \frac{h^*}{\sqrt{\mu^2/\rho_a p_a}} \qquad \text{Dimensionless gap} \qquad (38e)$$

$$P_k = \frac{k}{p_a} \qquad \text{Dimensionless stiffness per unit width} \qquad (38f)$$

$$P_c = \frac{c}{\mu} \qquad \text{Dimensionless damping coefficient per unit width} \qquad (38g)$$

$$P_f = \frac{\mu f}{p_a} \qquad \text{Dimensionless frequency} \qquad (38h)$$

$$P_\omega = \frac{r_o \omega}{U} \qquad \text{Frequency ratio} \qquad (38i)$$

For the case of no radial load ($x_s = y_s = 0$), the equilibrium tension, gap, stiffness, and damping parameters can be expressed as follows:

$$P_{T_s} = P_{T_s}\left(P_{T_o}, P_\ell, \Omega, P_u, P_r\right) \qquad (39)$$

$$P_h = P_h\left(P_{T_o}, P_\ell, \Omega, P_u, P_r\right) \qquad (40)$$

$$P_k = P_k\left(P_{T_o}, P_\ell, \Omega, P_u, P_r, P_f\right) \qquad (41)$$

$$P_c = P_c\left(P_{T_o}, P_\ell, \Omega, P_u, P_r, P_f\right) \qquad (42)$$

In the graphical presentation of results, values of pertinent dimensionless parameters and of corresponding characteristic physical variables are stated next to each curve. This dual representation is intended to facilitate the physical interpretation of the results. In selecting the sample values, the following magnitudes of physical parameters have been used:

p_a = 14.7 psi

ρ_a = 0.075 lb-in/ft^3

μ = 0.265 x 10^{-8} lbf-sec/in^2

E = 30 x 10^6 psi

ℓ_o / r_o = 1.985

The effect of variation of speed, initial tension, foil thickness, journal radius and wrap angle on the steady-state tension of the foil are shown in Fig. 3 and follow the intuitively anticipated trend. The same holds true for the gap width in Fig. 4. In Fig. 5, the stiffness coefficient is shown to increase with frequency in an undulatory fashion to an asymptotic value. Analogously, the damping coefficient is shown to decrease to zero with frequency in an undulatory manner. (See Fig. 6) It is particularly noteworthy that no sensitivity to excitation at half the rotational frequency is exhibited.

The asymptotic and the undulatory behavior is discussed below. In order to be specific, the approximation is made that the major contribution to foil length variations stems from the central region. (i.e. B = 0 in Eq. (31).)

Each frame in Fig. 7 shows perturbations of gap width at four sample time points, $\omega t = 0, 0.5\pi, \pi, 1.5\pi$. It can be seen that the higher the exitation frequency the greater the number of waves within the region of wrap. The latter travel at approximately U/2 from the inlet to the exit as shown analytically [11] and verified experimentally by Licht [15]. The wave transit time from inlet to exit is approximately $2\Theta r_o/U$. With the period of exitation $2\pi/\omega$, the condition that an integral number of waves be contained within the region of wrap is:

$$P_\omega \equiv \frac{\omega}{U/r_o} = \frac{\pi j}{\Theta} \qquad j = 1, 2, \ldots \qquad (43)$$

For the particular case shown in Fig. 7, $\Theta = \pi/3$. For a frequency ratio of $P_\omega = 3$, one full wave is seen to be present in the region of wrap. For $P_\omega = 6$, two full waves are accommodated and so forth.

When an integral number of waves is present with ω one can write approximately:

$$\int_{-\Theta/(2\epsilon^{1/3})}^{\Theta/(2\epsilon^{1/3})} f\,d\xi = \int_{-\Theta/(2\epsilon^{1/3})}^{\Theta/(2\epsilon^{1/3})} \tilde{f}\,d\xi = \int_{-\Theta/(2\epsilon^{1/3})}^{\Theta/(2\epsilon^{1/3})} \tilde{h}\,d\xi \tag{44}$$

It follows that for frequencies given by Eq. (43) the right hand side of Eq. (31) is real. Consequently, the damping coefficient vanishes for these frequencies and the stiffness coefficient is essentially the same for all values of j. Hence the undulatory behavior. Approximate stiffness formulae are given in Appendix A.

The fact that the damping constant vanishes at discrete frequencies, denoted as "critical", has an important design implication. If the rotor mass is such that resonance occurs at one of the critical frequencies, the resonance is undamped. In reality, some external damping will exist in the system, but the critical frequencies may nevertheless, be dangerous. "Critical" values of mass should, therefore, be avoided in design. For example, using the approximate value of stiffness given in Eq. (A10) of the Appendix, the critical mass, based on the lowest frequency at which damping vanishes, is:

$$m_c \cong \frac{6 \sin^2\frac{\Theta}{2}\, T_s\, \epsilon^{-2/3}\, r_o}{\left(\frac{T_s}{Ed}\frac{l_o}{r_o}\epsilon^{-2/3} + \frac{H^*\,\Theta}{1+C}\right)\left(\frac{\pi U}{\Theta}\right)^2} \tag{45}$$

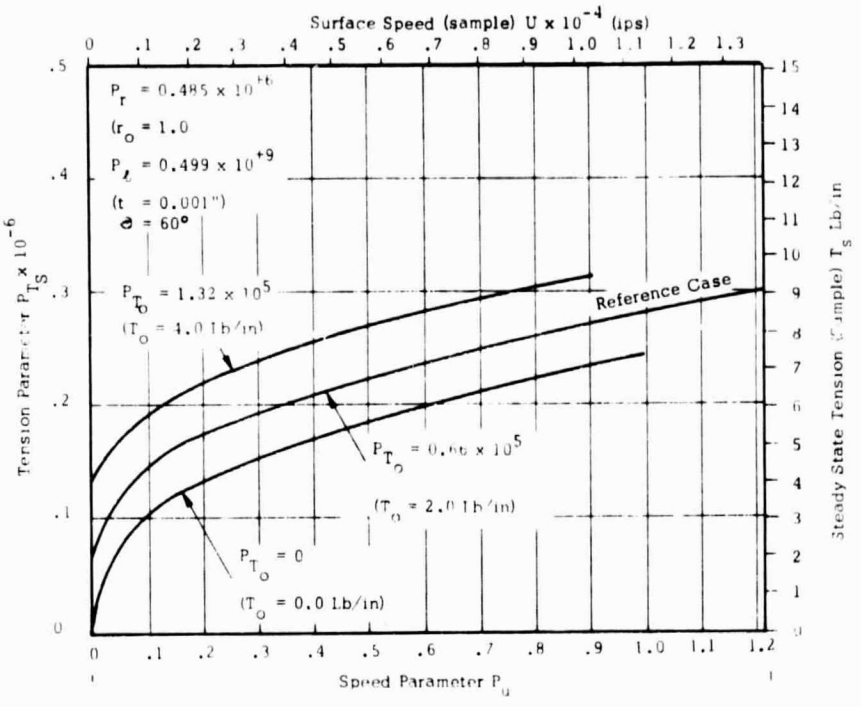

Fig. 3a Effect of Initial Tension on Steady State Tension

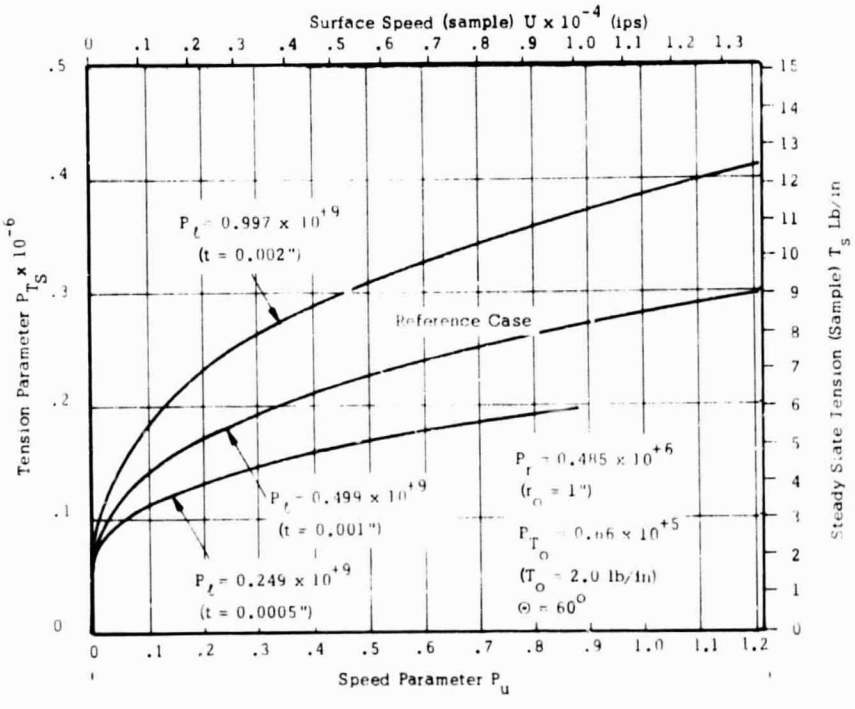

Fig. 3b Effect of Foil Thickness on Steady State Tension

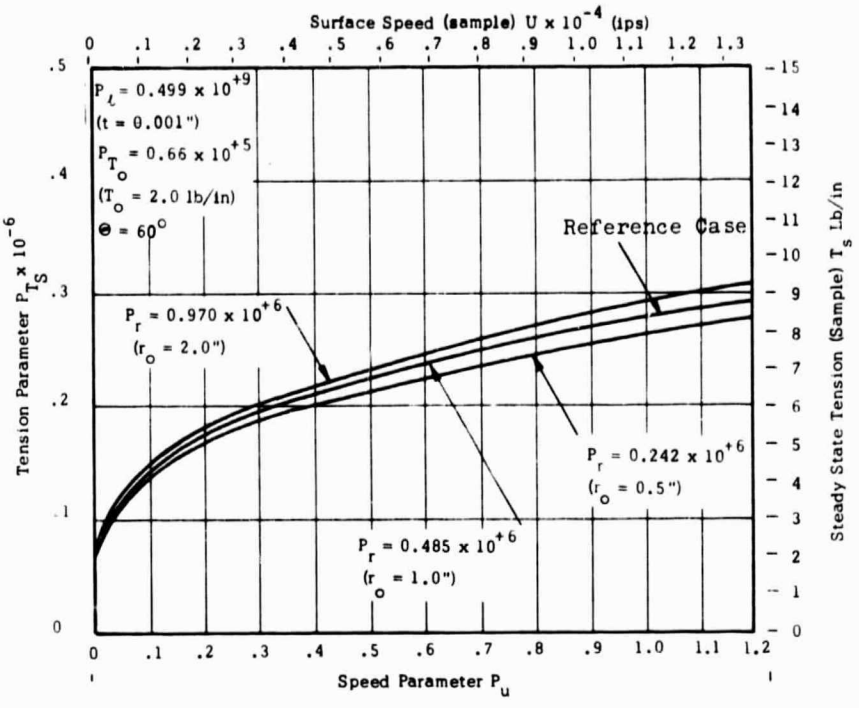

Fig. 3c Effect of Journal Radius on Steady State Tension

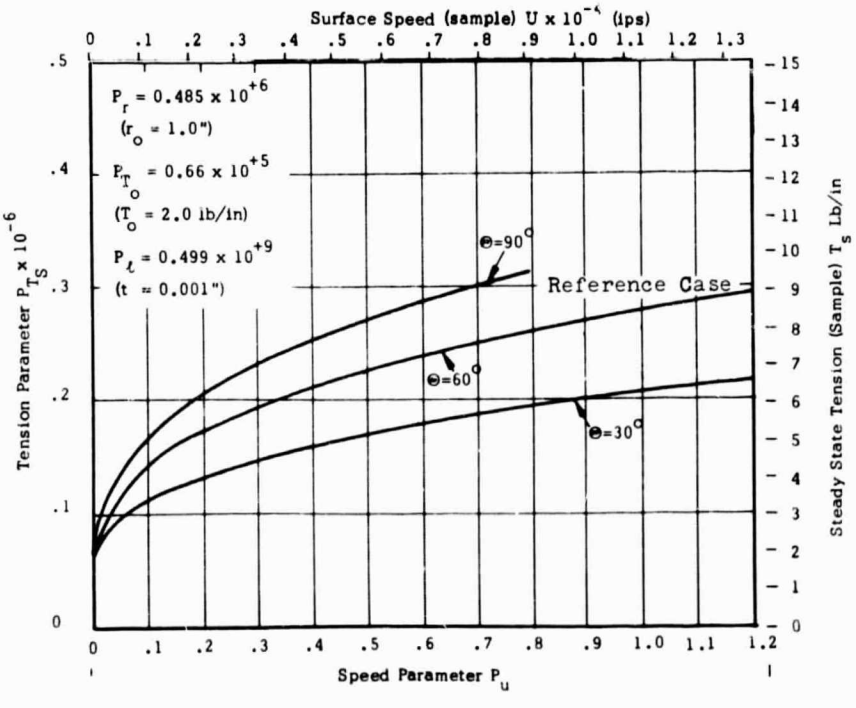

Fig. 3d Effect of Wrap Angle on Steady State Tension

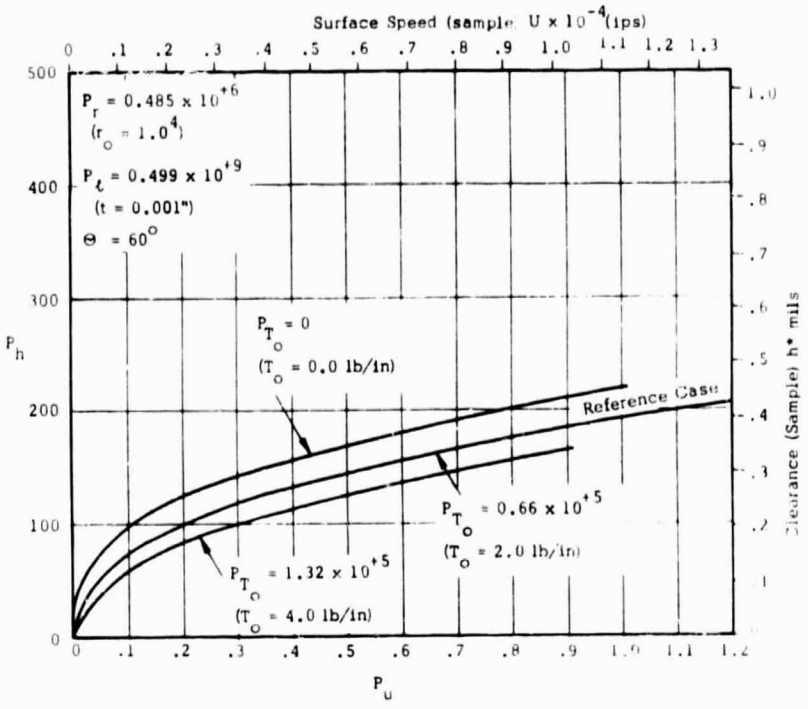

Fig. 4a Effect of Initial Tension on Steady State Clearance

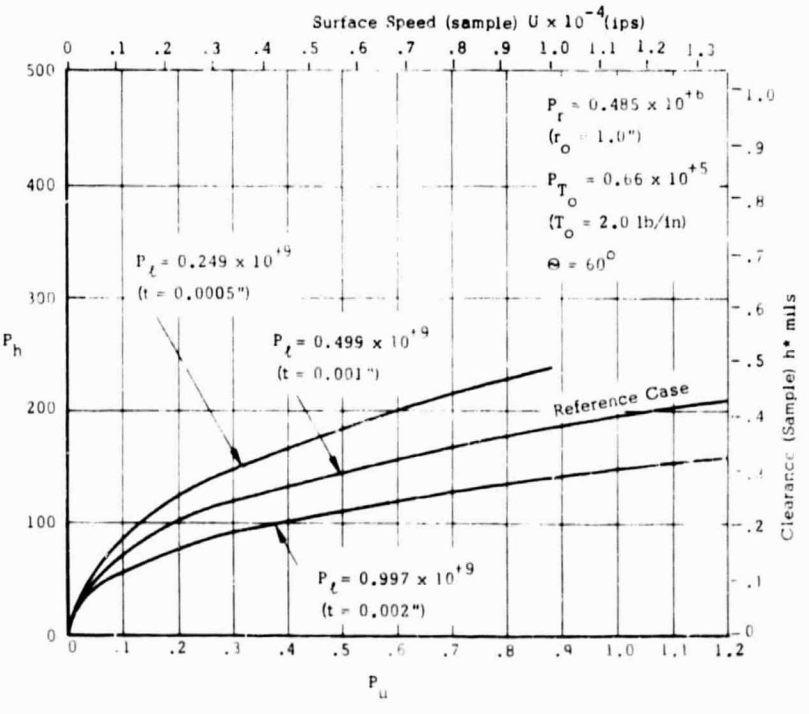

Fig. 4b Effect of Foil Thickness on Steady State Clearance

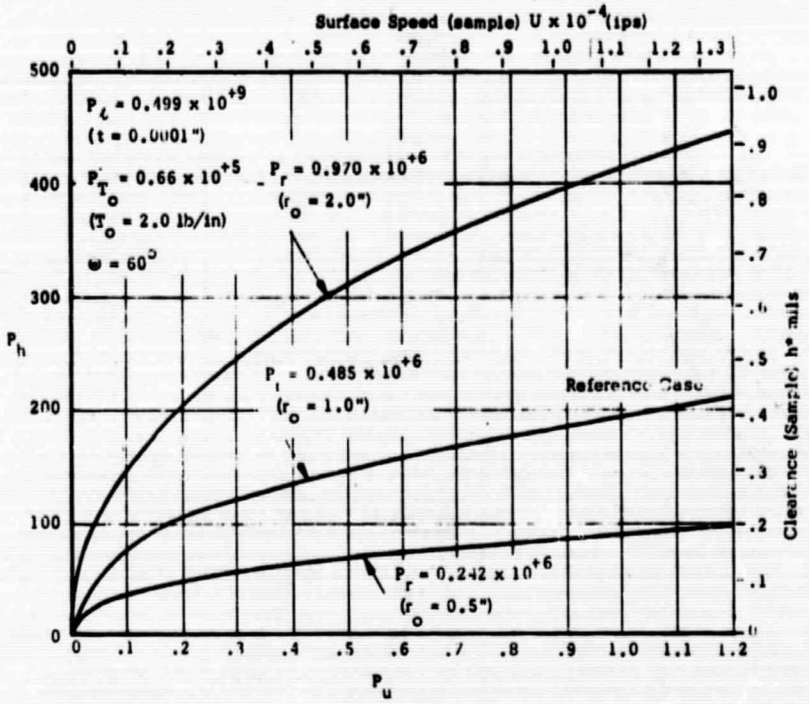

Fig. 4c Effect of Journal Radius on Steady State Clearance

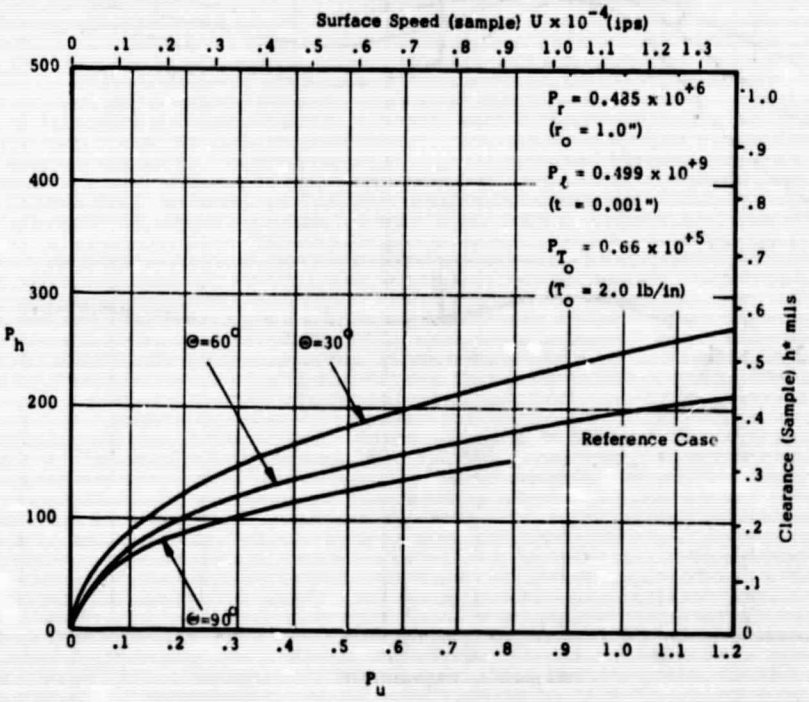

Fig. 4d Effect of Wrap Angle on Steady State Clearance

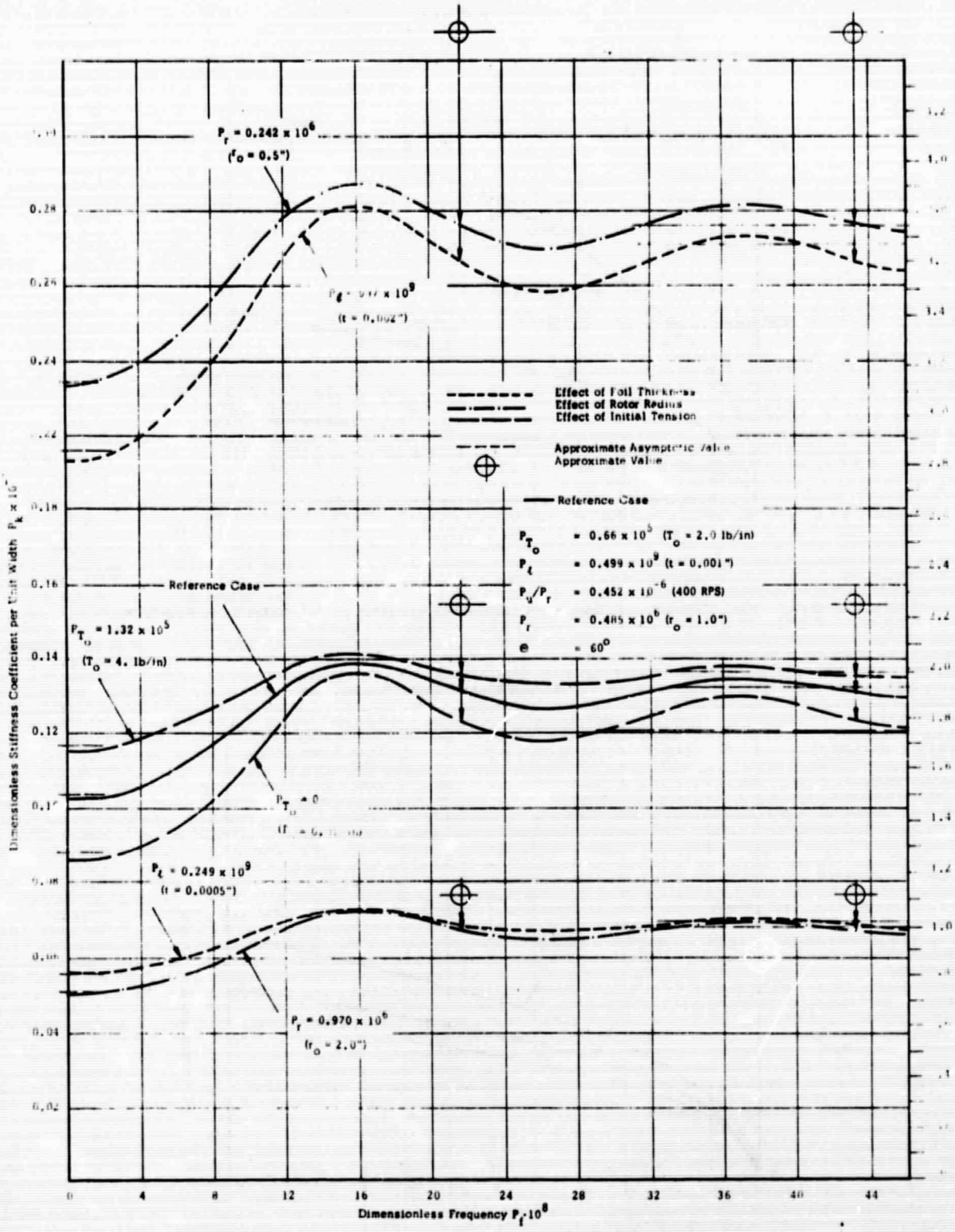

Fig. 5a Stiffness Coefficient as a Function of Excitation Frequency

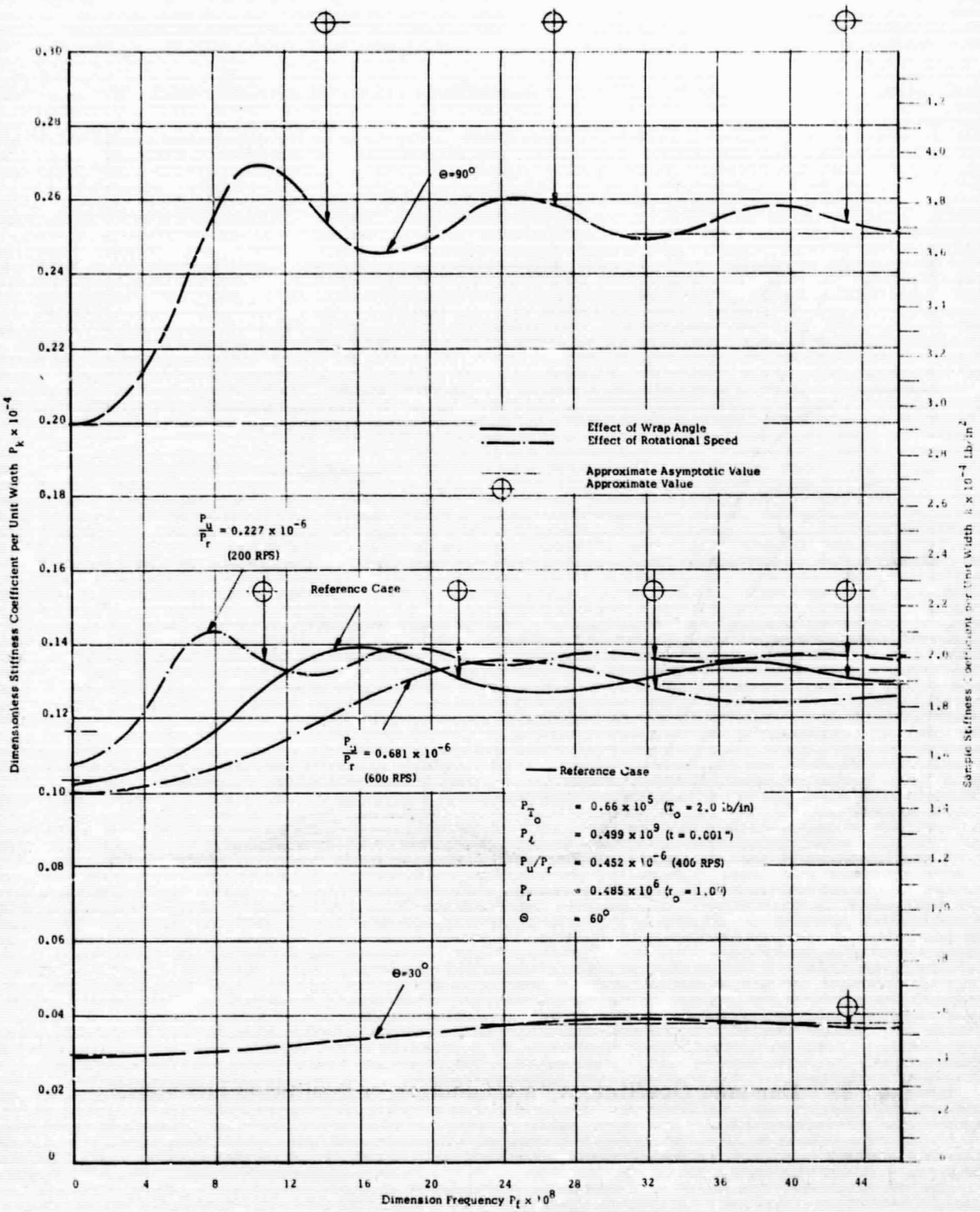

Fig. 5b Stiffness Coefficient as a Function of Excitation Frequency

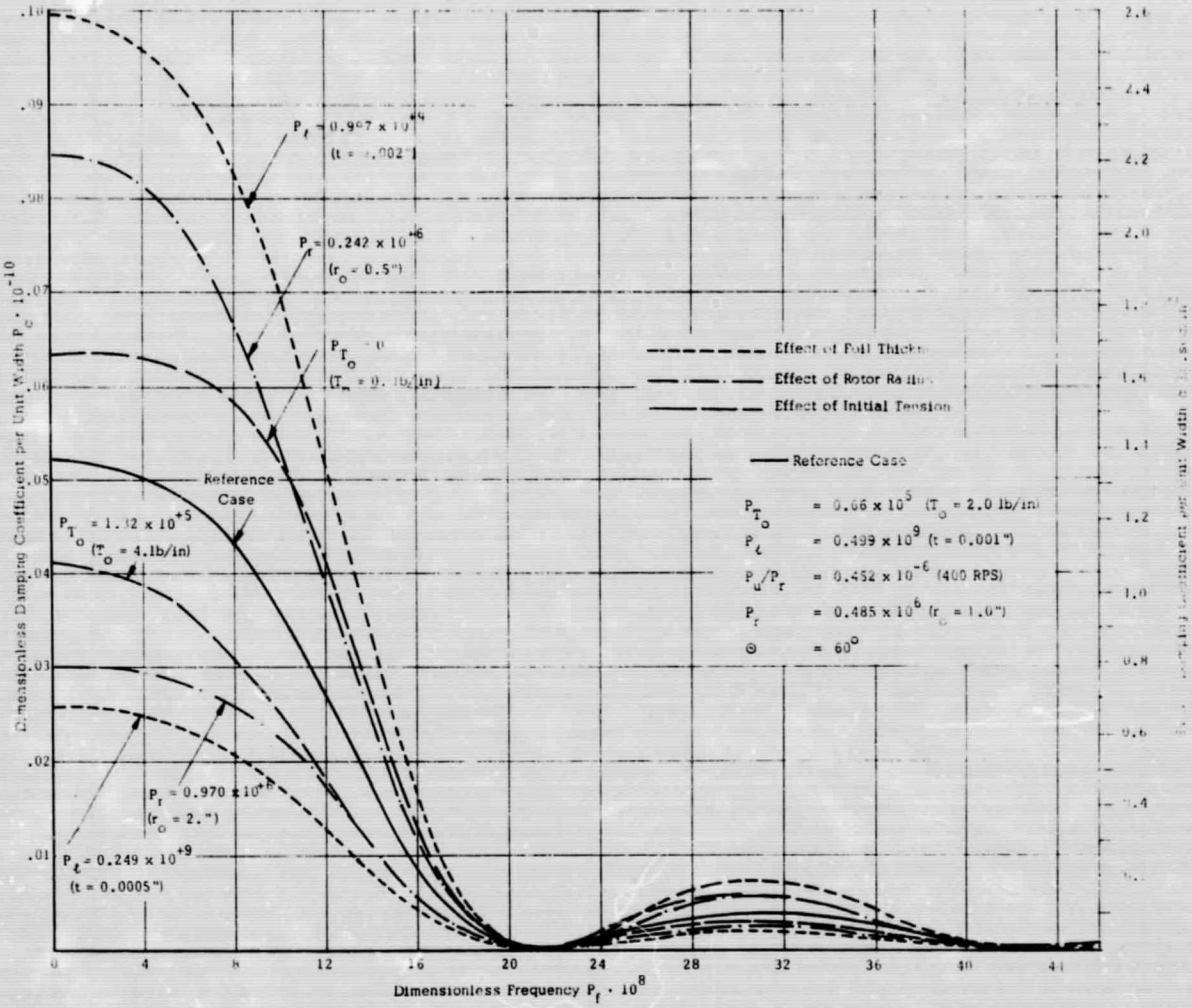

Fig. 6a Damping Coefficient as a Function of Excitation Frequency

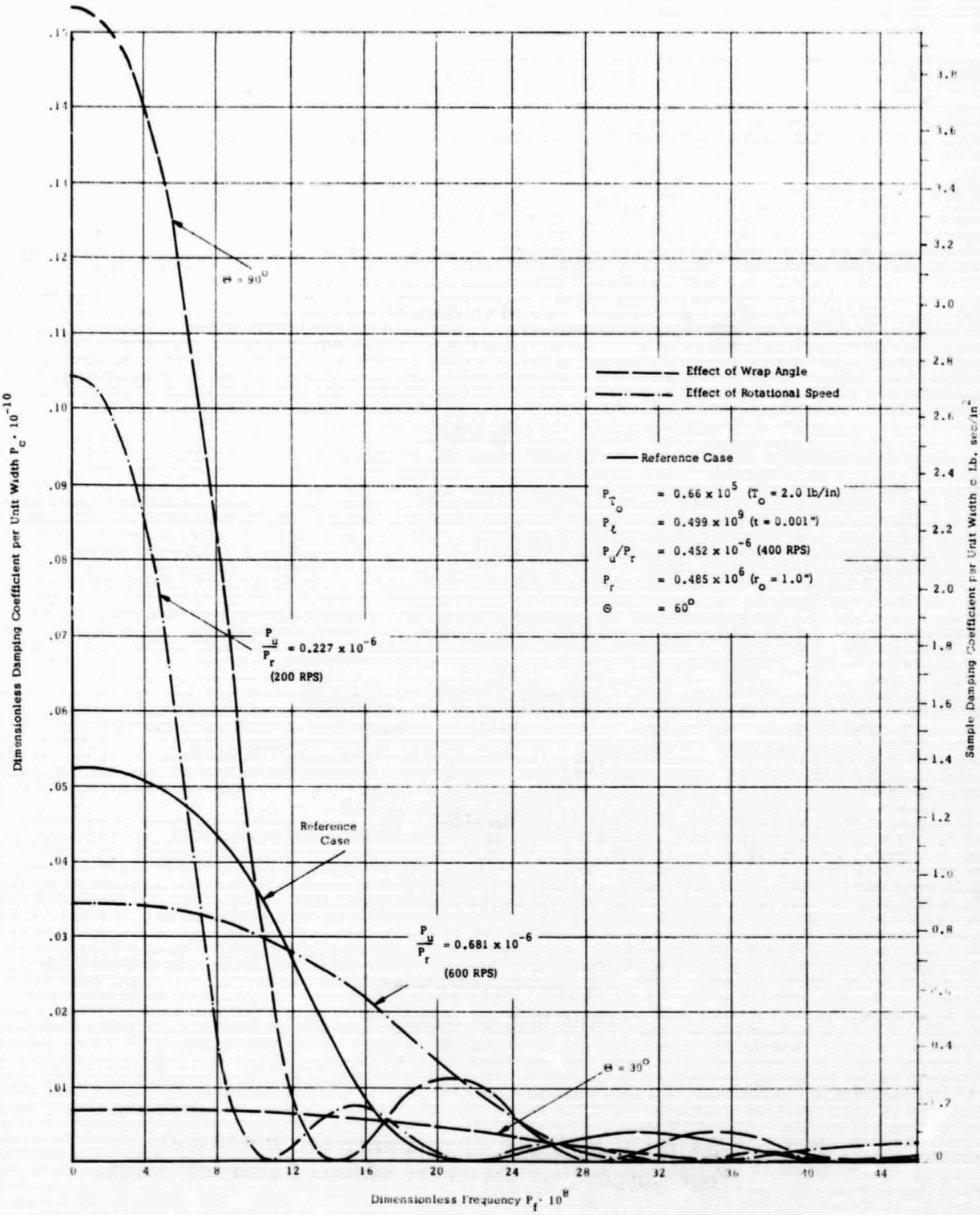

Fig. 6b Damping Coefficient as a Function of Excitation Frequency

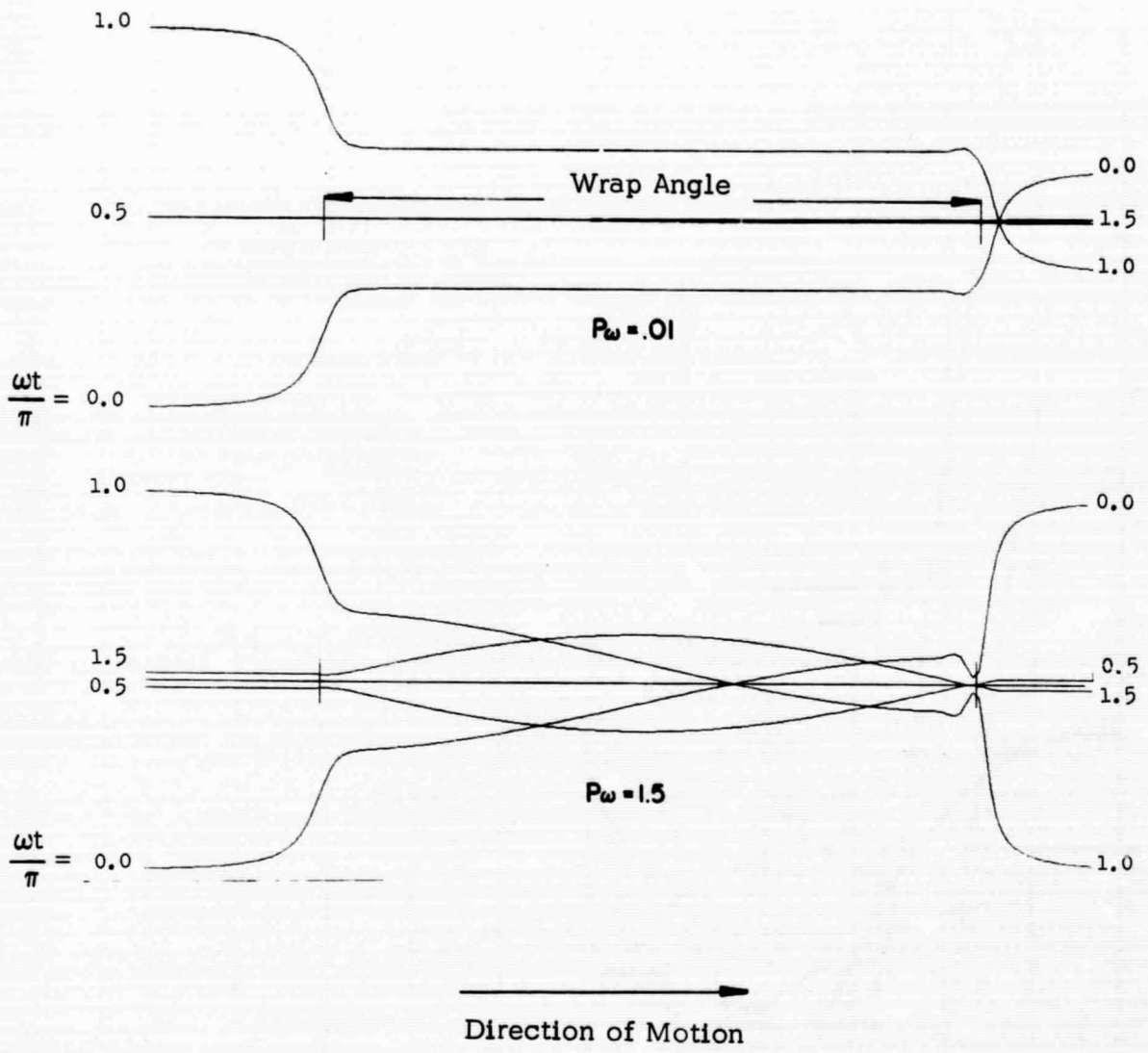

Fig. 7 Spatial distribution of clearance perturbation at four sample time points for various frequency ratios.

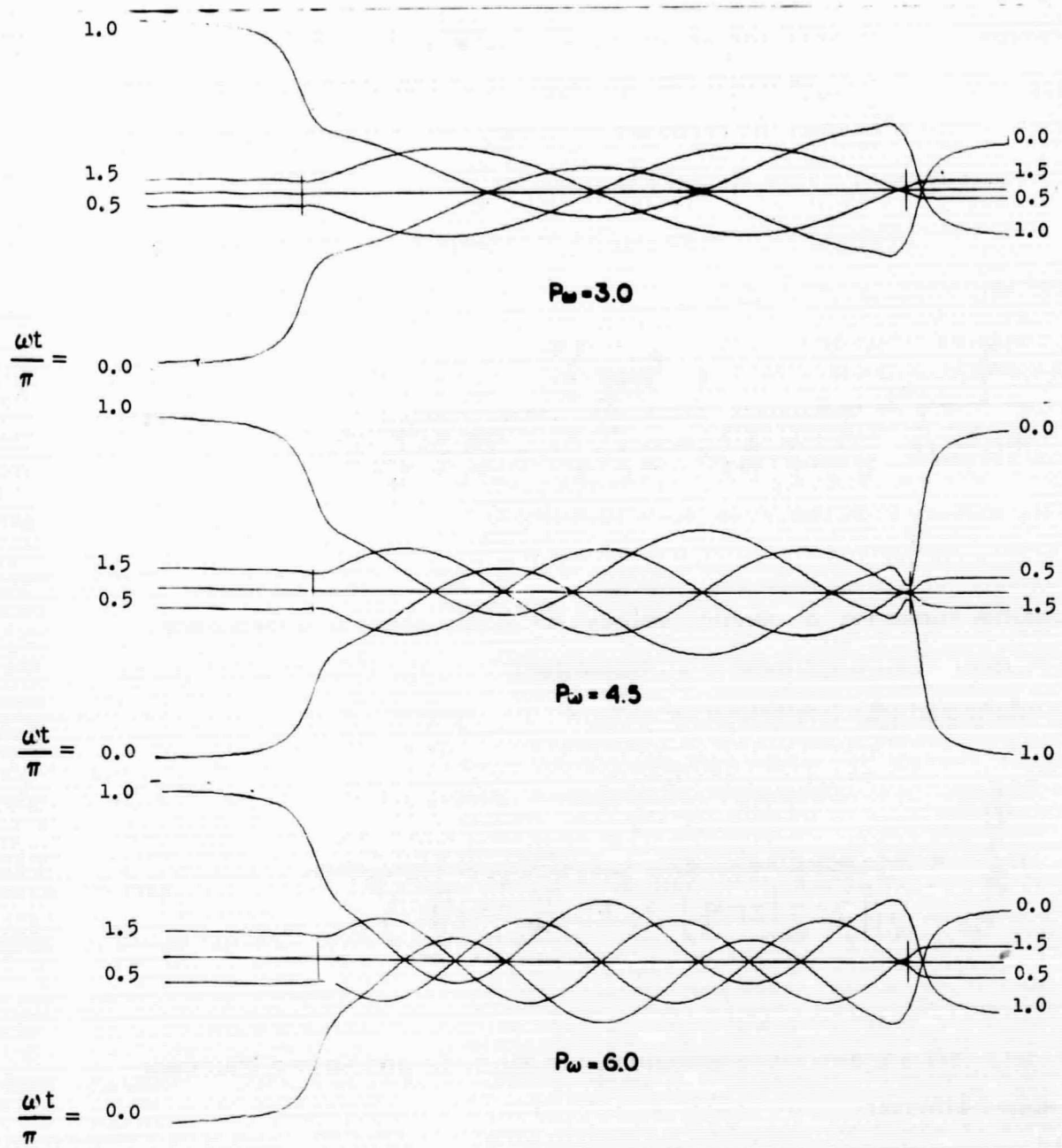

Fig. 7 Spatial distribution of clearance perturbation at four sample time points for various frequency ratios. (cont).

Additional critical mass values are $m_c/2^2$, $m_c/3^2$, etc. Referring to Fig. 5 and 6, it will be noted that an increase in the rotor mass above the critical value will shift the resonant frequency into a region in which film damping is higher. This practice is recommended.

In the case of response to imbalance m·e, the "amplitude ratio" is

$$\frac{\tilde{\eta}}{me\omega_c^2/k} = \frac{\left(P_f/P_{fc}\right)^2}{\sqrt{\left(\left[\frac{c}{\mu}/\frac{k}{p_a}\right]2\pi P_f\right)^2 + \left(1 - \frac{m}{m_c}\frac{k_c}{k}\frac{P_f^2}{P_{fc}^2}\right)^2}} \tag{46}$$

Where the subscript c denotes values at the lowest critical frequency. The ratio of shaft amplitude to static deflection in the case of response to a constant periodic excitation is:

$$\frac{\tilde{\eta}}{\tilde{\eta}_{st}} = \frac{1}{\sqrt{\left(\left[\frac{c}{\mu}/\frac{k}{p_a}\right]2\pi P_f\right)^2 + \left(1 - \frac{m}{m_c}\frac{k_c}{k}\frac{P_f^2}{P_{fc}^2}\right)^2}} \tag{47}$$

Eq. (46), (47) are described graphically in Figs. 8a and 8b and illustrate the above effects.

At high frequency the stiffness approaches a constant value while damping tends to zero. Again, this is what one would expect as the film becomes locally trapped in the gap, without appreciable side flow. Approximate values of stiffness in the limits of low and high frequencies are given in Appendix A and are indicated in Figs. 5 and 6. The approximate values are in good agreement with those based on more exact calculations.

One essential factor missing in the present formulation is the effect of fluid inertia. This effect is very important [10], and further work is in progress to account for its influence. Because of this deficiency, the results given herewith are accurate for low speeds of rotation, but may serve as a guide in conjunction with results reported in reference [10].

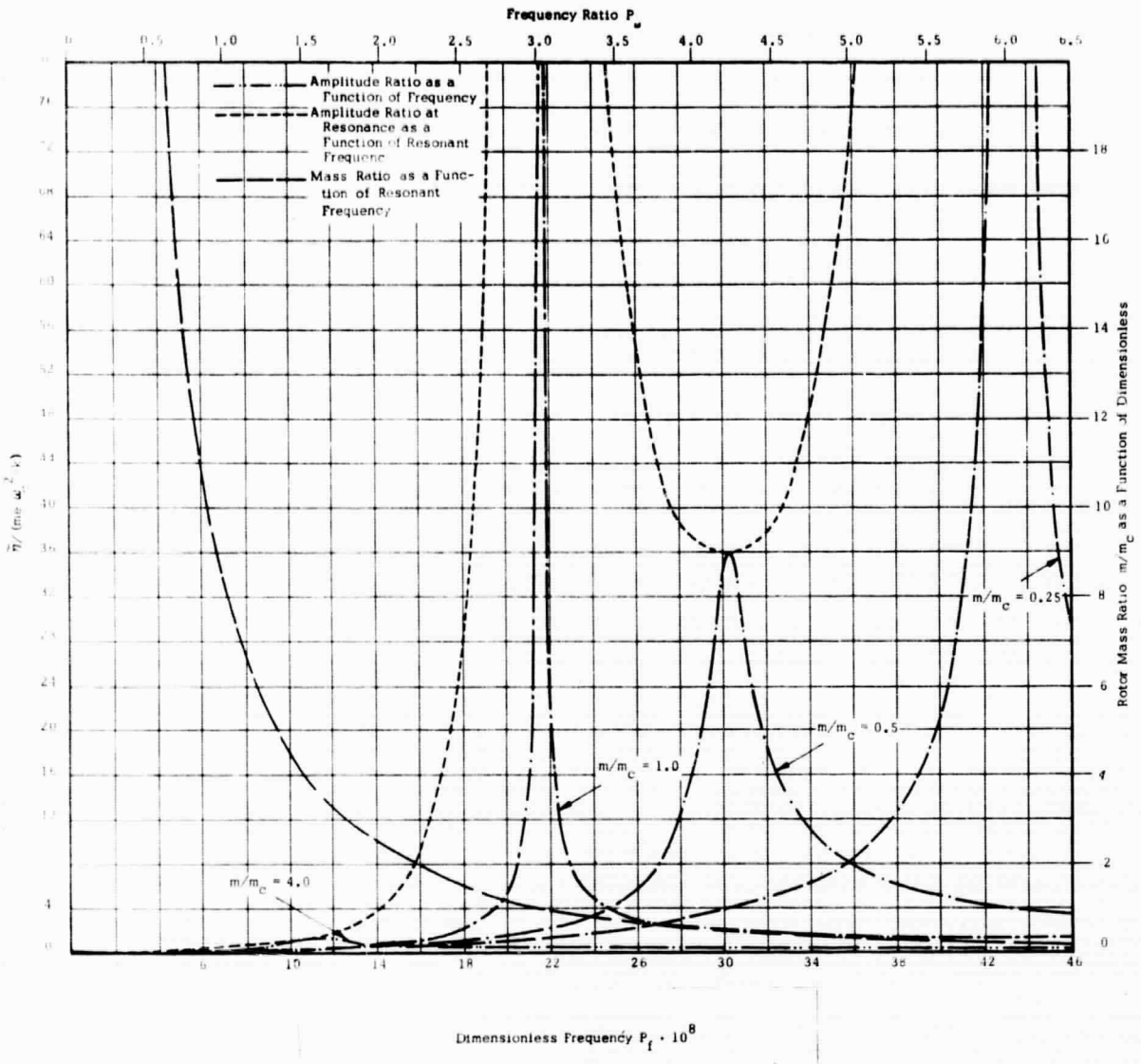

Fig. 8a Frequency Response to Rotating Imbalance With Rotor Mass as a Parameter

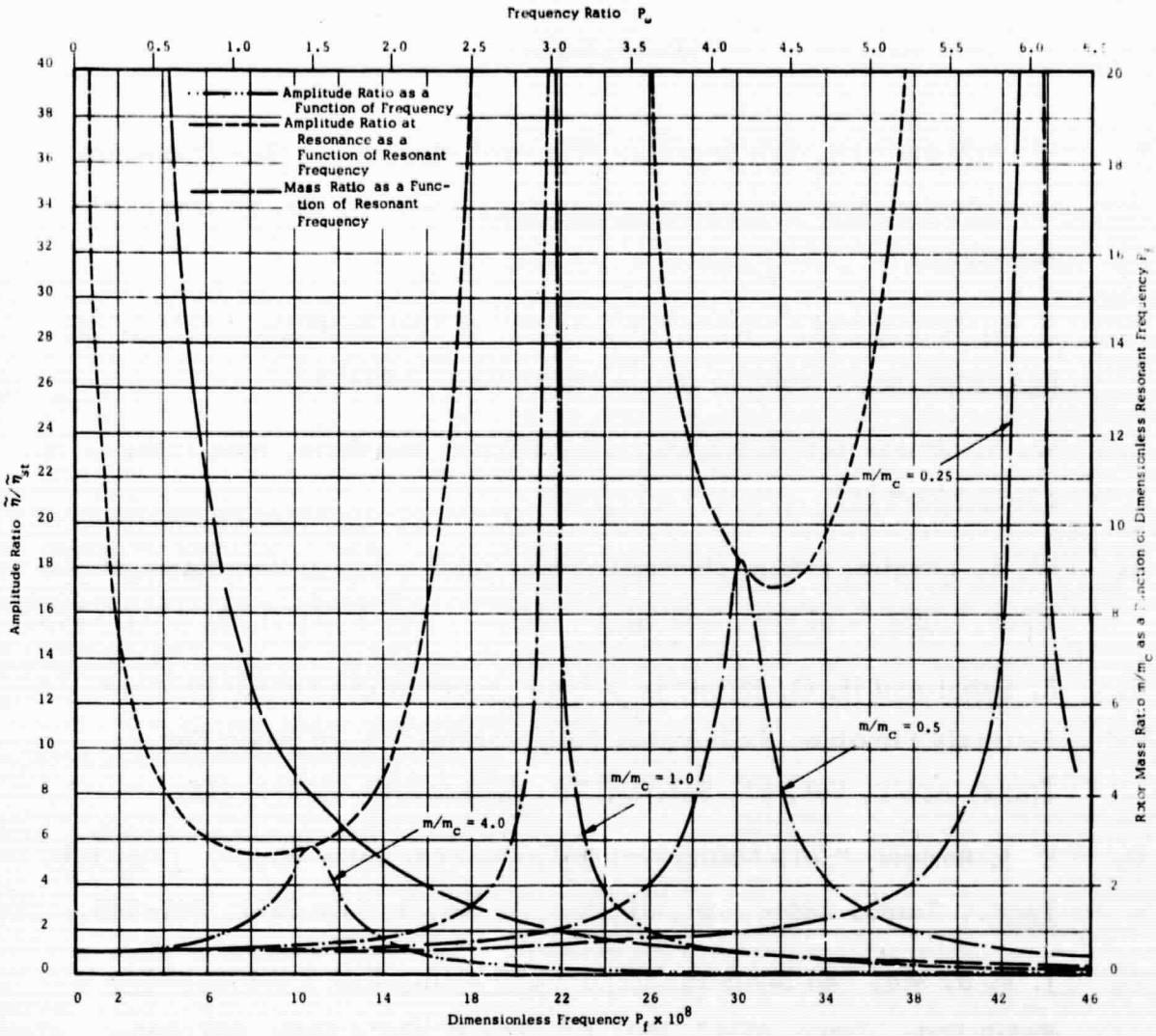

Fig. 8b Frequency Response to a Constant Periodic Excitation With Rotor Mass as a Parameter

REFERENCES

1. H. Blok and J. J. Van Rossum, "The Foil Bearing - A New Departure in Hydrodynamic Lubrication," Lub Eng., Vol. 9, No. 6, Dec. 1953, 316-320.

2. H. K. Baumeister, "Nominal Clearance of Foil Bearings," IBM J. of Res. and Dev., Vol. 7, No. 2, April 1963, 153-154.

3. W. A. Gross, Gas Lubrication, John Wiley and Sons, New York, 1962, 138-141.

4. W. E. Langlois, "The Lightly Loaded Foil Bearing at Zero Angle of Wrap," IBM J. of Res. and Dev., Vol. 7, No. 2, April 1963, 112-116.

5. A. Eshel and H. G. Elrod, Jr., "The Theory of the Infinitely Wide, Perfectly Flexible, Self-Acting Foil Bearing," J. of Basic Eng., Trans. ASME, Vol. 87, Ser. D, No. 4, Dec. 1965, 831-836.

6. E. J. Barlow, "Self-Acting Foil Bearings of Infinite Width," J. of Lub. Tech., Trans. ASME, Vol. 85, Ser. F, No. 3, July 1967, 341-345.

7. J. T. S. Ma, "An Investigation of Self-Acting Foil Bearings," J. of Basic Eng., Trans. ASME, Vol. 87, No. 4, Dec. 1965, 837-846.

8. L. Licht, "An Experimental Study of Elasto-Hydrodynamic Lubrication of Foil Bearings," J. of Lub. Tech. Trans. ASME, Vol. 90, Ser. F, No. 1, 1968, 199-220.

9. E. J. Barlow, Internal Ampex Corporation Communication.

10. L. Licht and A. Eshel, "Study, Fabrication and Testing of a Foil Bearing Rotor Support System," NASA Report CR-1157, Nov. 1968.

REFERENCES (Cont)

11. A. Eshel and M. Wildmann, "Dynamic Behavior of a Foil in the Presence of a Lubricating Film," J. of Appl. Mech., Trans. ASME, Vol. 35, June 1968, 242-247.

12. T. Barnum and H. G. Elrod, Jr., "A Theoretical and Experimental Study of the Dynamic Behavior of Foil Bearings," Columbia University, Lubrication Laboratory Report 14, 1968.

13. C. H. T. Pan, "Spectral Analysis of Gas Bearing Systems for Stability Studies," Mechanical Technology Inc. Report 64TR58, 1964.

14. V. Castelli and H. G. Elrod, Jr., "Solution of the Stability Problem for 360 Degree Self Acting, Gas Lubricated Bearings," ASME paper 64-Lubs-10.

15. L. Licht, "On the Velocity of Propagation of a Disturbance Along a Foil" J. of App. Mech., Trans. ASME, Vol. 36, June 1969.

APPENDIX A

APPROXIMATE TREATMENT OF LIMITING CONDITIONS

It is possible to obtain in a simple manner, approximate results for certain limiting cases. If one limits attention to the central region, where the equilibrium solution predicts uniformity of clearance, Eq. (27a), when written in terms of the variable defined in Eq.(30) becomes:

$$\frac{d^4\tilde{h}}{d\xi^4} H^{*3}(1+C) - \frac{d^3\tilde{h}}{d\xi^3} H^* - \frac{d^2\tilde{h}}{d\xi^2} S H^* + \frac{d\tilde{h}}{d\xi}(1+C) + \tilde{h} S (1+C) = -S H^* \quad \text{(A1)}$$

In addition, a simplified relation between tension fluctuations and shaft excursions is obtained by substituting B=0 in Eq. (31)

$$\frac{\tilde{\varphi}_k}{\tilde{\eta}_k} = \frac{2 \sin \frac{\Theta}{2}}{-\frac{T_{sk}}{Ed}\frac{l_o}{r_o}\epsilon_k^{-2/3} + \epsilon_k^{1/3} \int_{-\Theta/(2\epsilon^{1/3})}^{\Theta/(2\epsilon^{1/3})} \tilde{h}_k \, d\xi} \quad \text{(A2)}$$

When $\tilde{h}_k$ is known in the uniformity region, Eq. (A2) can be evaluated. Two extreme cases will be discussed below.

Quasi Static Limit

The solution of (A1) is composed of a linear combination of four exponential terms (corresponding to the roots of the characteristic equation of the homogeneous part of (A1)) plus a particular integral. A study of these solutions [12] reveals that three of them are insignificant in the central region whereas the fourth root of the characteristic equation can be expressed in the limit of small frequencies as

$$m = -\nu^4 - i\nu$$

Consequently, $\tilde{h}$ assumes in the central region and in the limit of low frequencies the form

$$\tilde{h}(\xi) = A e^{-(\nu^4 + i\nu)\xi} - \frac{H^*}{1+C} \qquad \text{(A3)}$$

where A is a complex coefficient. Since the disturbance is very slow one cannot expect any lag in the response. Thus, the imaginary part of $\tilde{h}$ (ξ) must vanish with $\nu \to 0$. Therefore, in the limit the perturbation is real and uniform throughout the central region. This is the usual situation, when for zero frequency there is no damping force, but nevertheless the damping coefficient does not necessarily vanish. The constant perturbation-amplitude may be found from the steady state solution

$$h^* = r_0 \left(\frac{6\mu U}{T_s}\right)^{2/3} H^* \qquad \text{(A4)}$$

where

$$H^* = H^* \left(\frac{p_a r_0}{T_s}\right)$$

Taking the differential, one finds

$$\tilde{h} = -\left(\frac{2}{3}H^* - \frac{1}{C}\frac{dH^*}{d(\frac{1}{C})}\right) \tag{A5}$$

Thus, Eq. (A2) becomes

$$\frac{\varphi_k}{\tilde{\eta}_k} = \frac{2\sin\frac{\omega}{2}}{-\frac{T_{sk}}{Ed}\frac{l_o}{r_o}\epsilon_k^{-2/3} - \omega\left(\frac{2}{3}H_k^* - \frac{1}{C_k}\frac{dH^*}{d(\frac{1}{C})}\right)} \tag{A6}$$

For the central position it follows from Eq. (34) that

$$\frac{k}{p_a} = \frac{6\sin^2\frac{\omega}{2}\,\epsilon^{2/3}}{C\left(\frac{T_s}{Ed}\frac{l_o}{r_o}\epsilon^{-2/3} + \omega\frac{2}{3}H^* - \omega\frac{1}{C}\frac{dH^*}{d(\frac{1}{C})}\right)} \tag{A7}$$

No information about the damping coefficient c can be found, however, from this consideration. The reason is that the damping coefficient is the limit of the ratio of damping force to the circular frequency as the circular frequency tends to zero. The evaluation of this limit requires knowledge of the damping force not only at $\omega = o$ but in its neighborhood. The above does not provide such information.

Very High Frequency Limit

The roots of the characteristic equation of (A1) in the limit of $\nu \to \infty$ imply that none of the homogeneous solutions of (A1) affect the uniformity region. Therefore, the limiting behavior in this region is

$$\tilde{h}(\xi) = -\frac{H^*}{1+c} \tag{A8}$$

Physically, this is the behavior encountered generally in gas bearings in the limit of high frequency i.e. local isothermal compression. Under these circumstances, Eq. (A2) becomes

$$\frac{\tilde{\varphi}_k}{\tilde{\eta}_k} = \frac{-2\sin\frac{\Theta}{2}}{\frac{T_{sk}}{Ed}\frac{l_o}{r_o}\epsilon_k^{-2/3} + \frac{H_k^*\Theta}{1+c_k}} \tag{A9}$$

In the central position the stiffness and damping coefficients become

$$\frac{k}{p_a} = \frac{6\sin^2\frac{\Theta}{2}\,\epsilon^{-2/3}}{c\,\frac{T_s}{Ed}\,\frac{l_o}{r_o}\,\epsilon^{-2/3} + \frac{H^*\Theta}{1+c}} \tag{A10}$$

$$\frac{c}{\mu} = 0 \tag{A11}$$

Case of $P_w = j\Theta/\pi \quad (j = 1, 2 \ldots)$

Under the above conditions, the number of wavelengths present within the angle of wrap is integral. Using Eq. (44), Eq. (31) becomes, approximately:

$$\frac{\tilde{\varphi}_k}{\tilde{\eta}_k} = \frac{2 \sin \frac{\Theta}{2}}{-\frac{T_{sk}}{Ed} \frac{l_o}{r_o} \epsilon_k^{-2/3}} \tag{A12}$$

In the central position the stiffness is then,

$$\frac{k}{p_a} = \frac{6 \sin^2 \frac{\Theta}{2}}{C \frac{T_s}{Ed} \frac{l_o}{r_o}} \tag{A13}$$

and the damping coefficient vanishes.

APPENDIX B

SOLUTION TECHNIQUE OF EQ. (27a)

The solution of Eq. (27a) is summarized below mainly for the sake of completeness. The equation was solved previously by Barnum and Elrod [12] and the technique used here is essentially the same.

The solution is obtained separately for the inlet, exit and central regions and matching conditions are applied. Eq. (27a) can be re-written in the form

$$\tilde{h}^{IV} F_{40}(\xi) + \tilde{h}''' F_{30}(\xi) + \tilde{h}'' \left[F_{20}(\xi) + i\nu F_{21}(\xi) \right] + \tilde{h}' F_{10}(\xi) + \tilde{h} \left[F_{00}(\xi) + i\nu F_{01}(\xi) \right] = \Phi_0(\xi) + i\nu \Phi_1(\xi) \tag{B1}$$

In the central region a simplified form of the coefficients is valid:

$$\frac{d^4\tilde{h}}{d\xi^4} - \frac{d^3\tilde{h}}{d\xi^3} \frac{1}{H^{*2}(1+C)} - \frac{d^2\tilde{h}}{d\xi^2} \frac{i\nu}{H^{*2}(1+C)} + \frac{d\tilde{h}}{d\xi} \frac{1}{H^{*3}} + \tilde{h} \frac{i\nu}{H^{*3}} = -\frac{i\nu}{(1+C)H^{*2}} \tag{B2}$$

The general solution of this equation is:

$$\tilde{h} = \sum_{1,4} A_j e^{m_j \xi / H^*} - \frac{H^*}{1+C} \tag{B3}$$

where m_j are the complex roots of the characteristic equation:

$$m^4 - \frac{m^3}{H^*(1+C)} - \frac{m^2(\nu H^*)}{H^*(1+C)} + m + (\nu H^*) = 0 \qquad \text{(B4)}$$

where m_j are the complex roots of the characteristic equation of (B2). The subscript j refers to the index shown in Fig. 9. The particular form of the solution desired for (B1) is such that it does not "blow up" in the central region. This implies that the complex coefficients A_3 and A_4 vanish for the representation of the central region as one approaches the inlet. It would imply further that A_1 and A_2 vanish in the representation of the central region as one approaches the exit. A_1 must, however, be retained for low frequencies due to the smallness of the real part of m and it thus provides the link between inlet and exit.

These restrictions on the form of behavior in the central region provide initial conditions for numerical integration of (B1) which is done separately toward the inlet and toward the exit. The remaining degrees of freedom (i.e. A_1 and A_2 for the inlet solution and A_3 and A_4 for the exit solution) must be determined from the boundary conditions, which state that far out in the inlet and in the exit regions

$$\tilde{h}' \to 0 \quad ; \quad \tilde{h}'' \to 0 \qquad \text{(B5)}$$

This is conveniently done for each region by generating numerically two linearily independent homogeneous solutions as well as a particular integral of (B1) and superposing them so that Eq. (B4) are satisfied.

In Fig. 10, sample curves of magnitude and phase of $\tilde{h}$ are shown as functions of frequency and may serve to further illustrate the dynamic behavior.

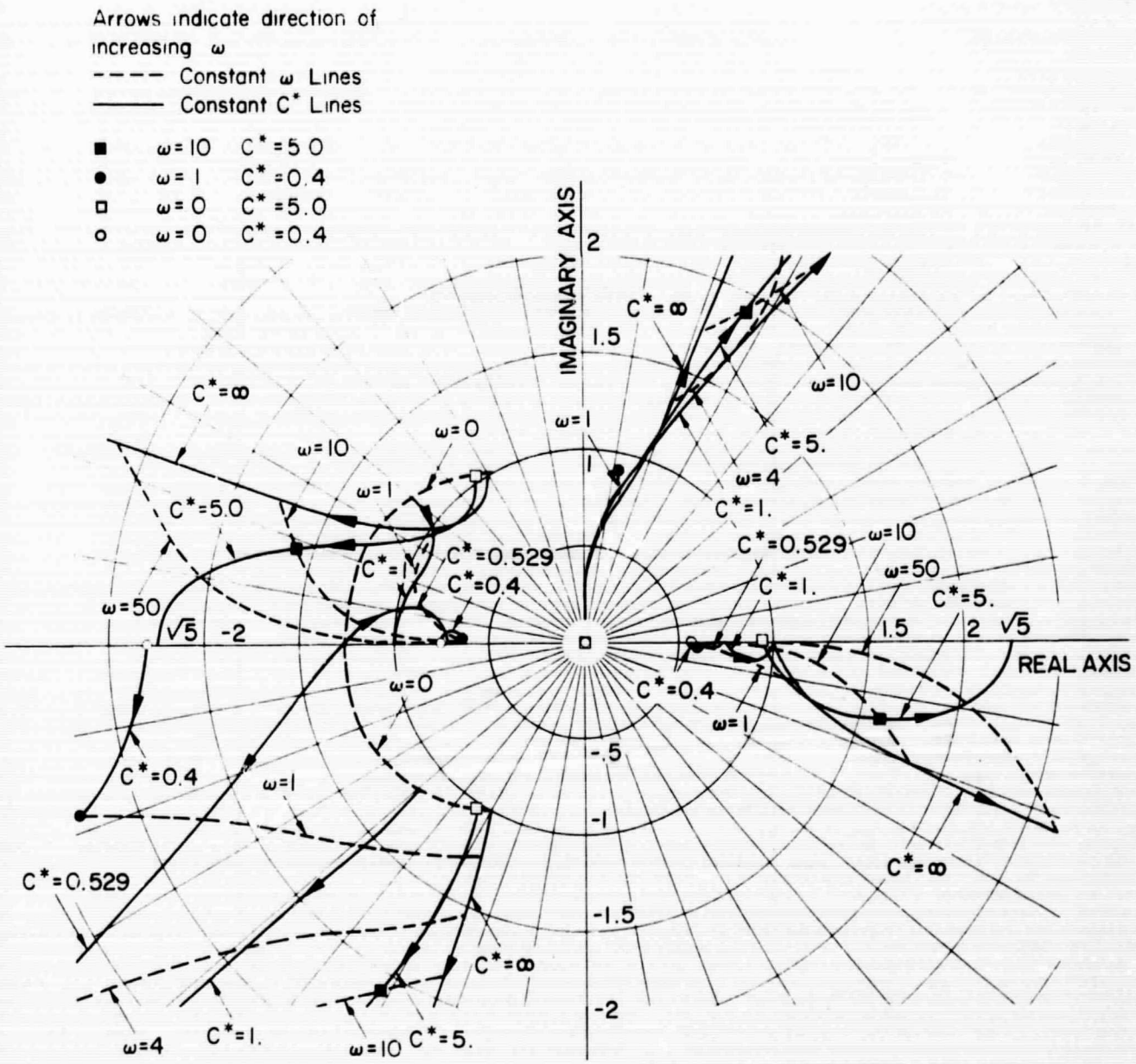

Fig. 9 Roots of the Characteristic Equation of (B2)

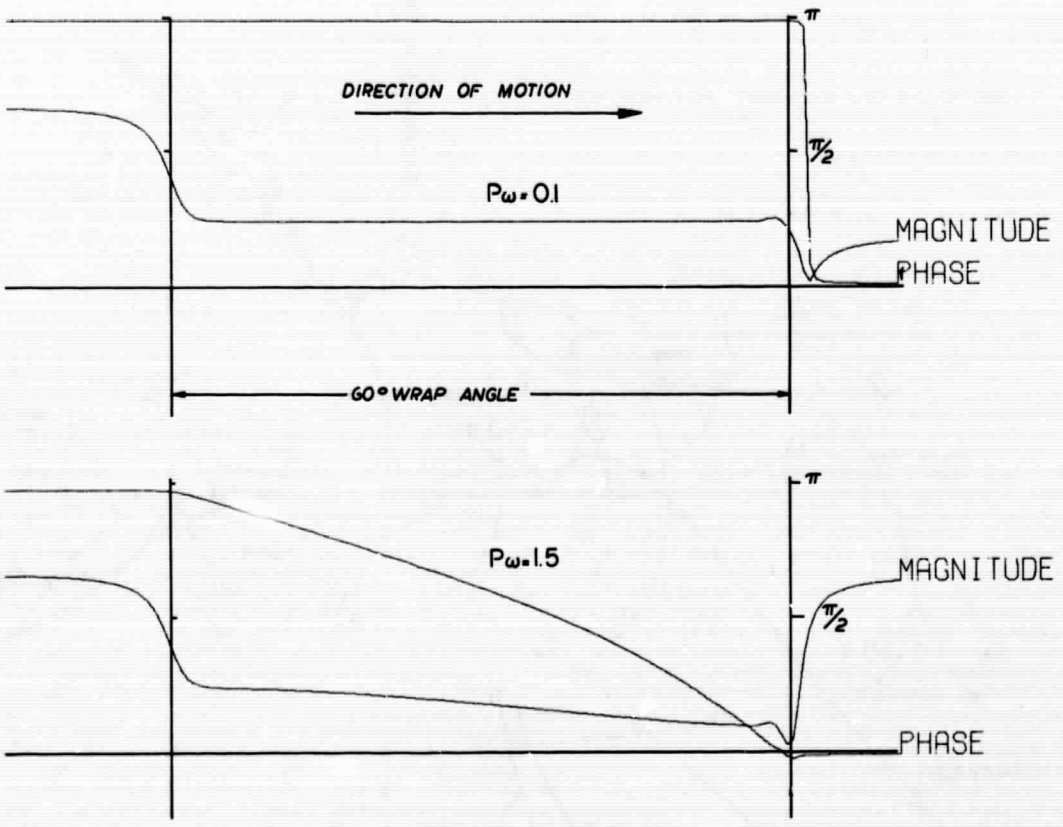

Fig. 10 Magnitude and Phase of Clearance Perturbation as a Function of Frequency Ratio P_ω

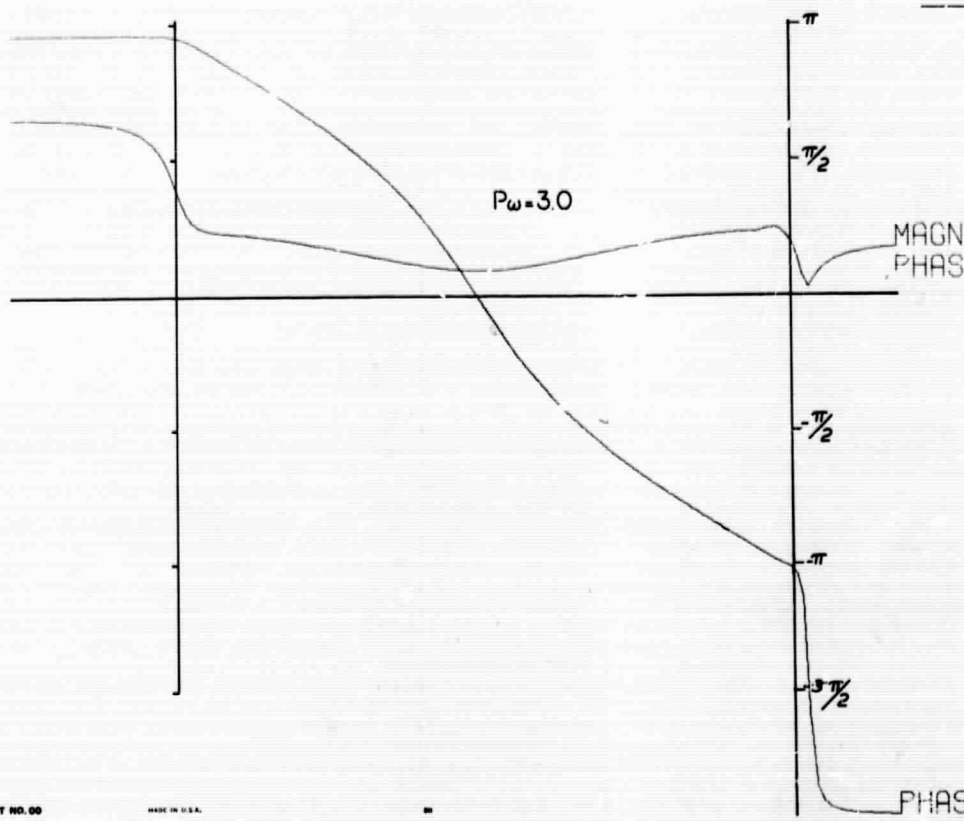

INC. ANAHEI ORNIA CHART NO. 00 MADE IN U.S.A.

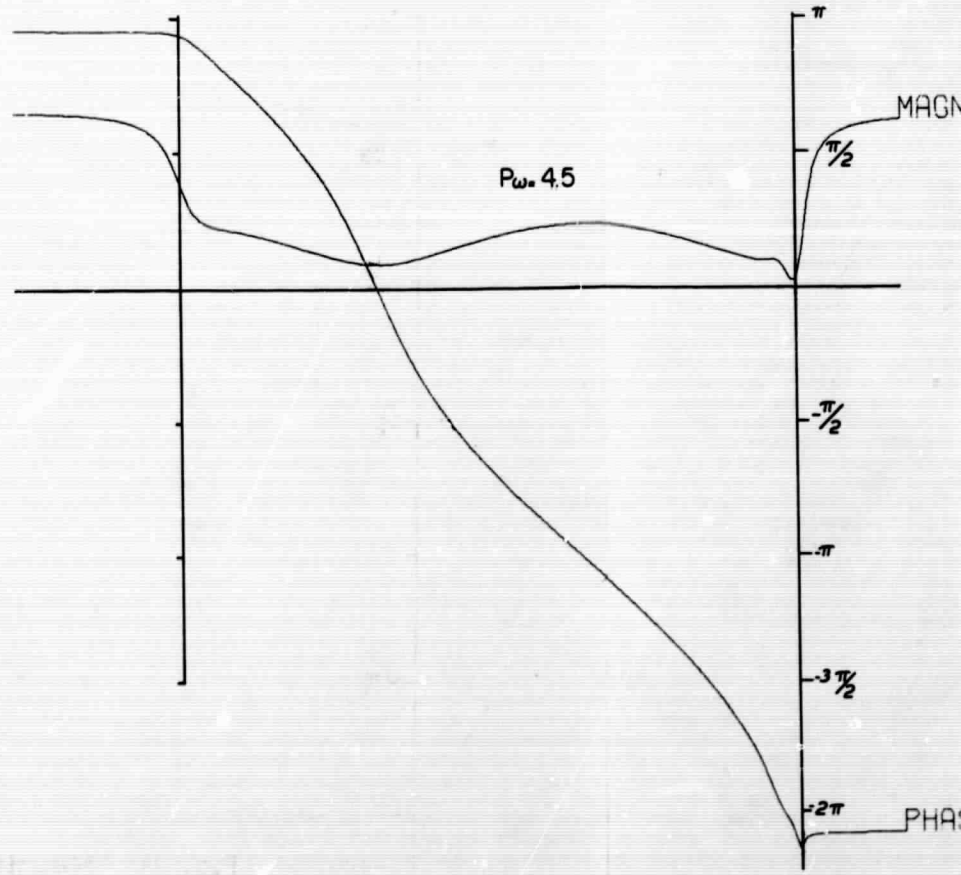

RR

FOLDOUT FRAME 1

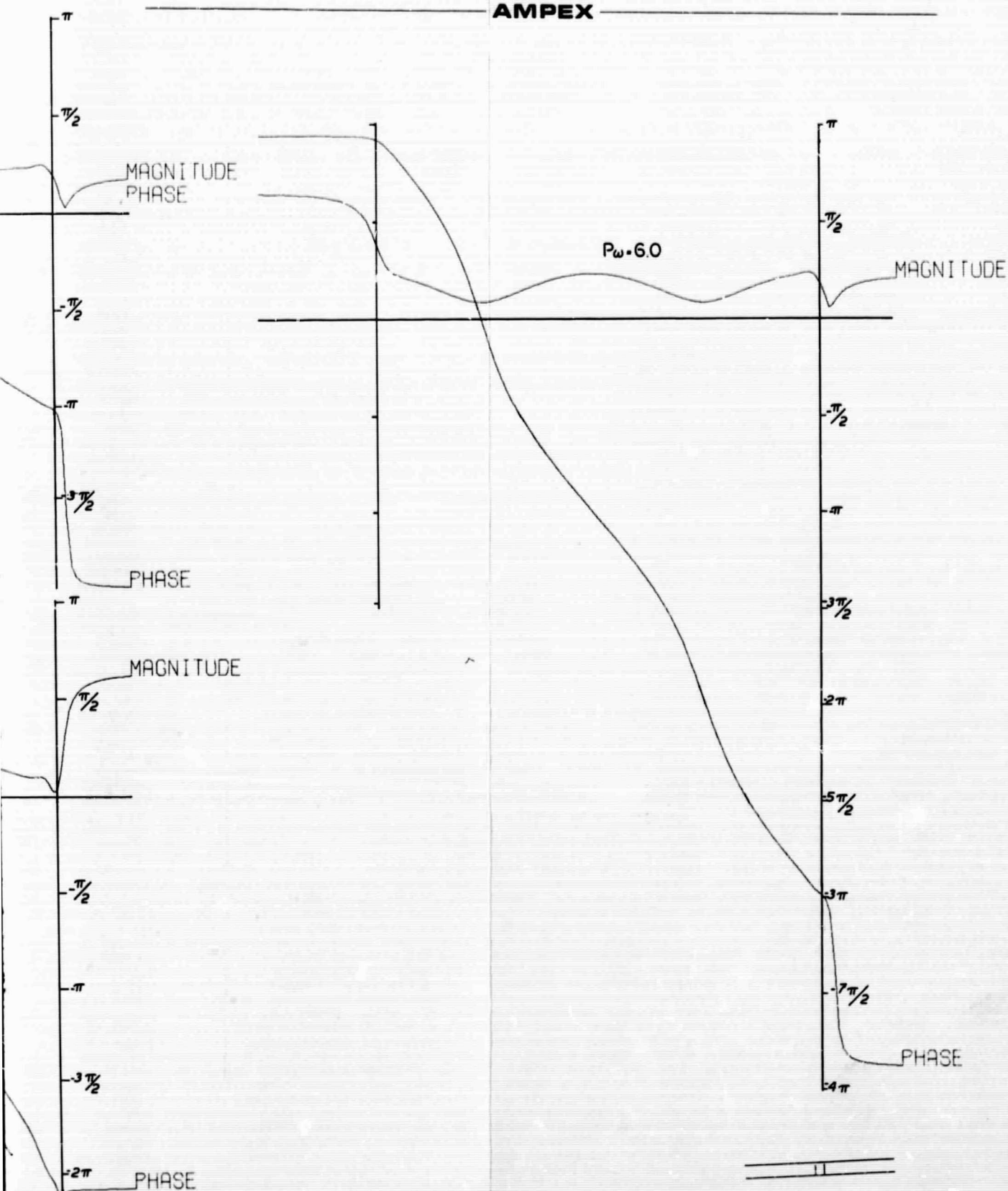

Fig. 10 Magnitude and Phase of Clearance Perturbation as a Function of Frequency Ratio P_ω (cont)